

479921 58-45

N93-11095

CHAPTER 8

P-49

Future Chlorine-Bromine Loading and Ozone Depletion

Authors:

M.J. Prather

A.M. Ibrahim

T. Sasaki

F. Stordal

G. Visconti

Model Contributors:

G.P. Brasseur

T. Sasaki

C.H. Bruehl

S. Solomon

D.A. Fisher

G. Visconti

I.S.A. Isaksen

D.J. Wuebbles

C.H. Jackman

E. Zhadin

M.K.W. Ko

S. Zvenigorodsky

Chapter 8

Future Chlorine-Bromine Loading and Ozone Depletion

Contents

SCIENTIFIC SUMMARY	8.1
8.1 INTRODUCTION.....	8.5
8.2 ATMOSPHERIC COMPOSITION AND CHEMISTRY	8.5
8.2.1 Lifetimes of the Halocarbons	8.6
8.2.2 Historical Record and Projections.....	8.7
8.2.3 Montreal Protocol: Halocarbon Scenarios	8.10
8.2.4 Gas Phase and Heterogeneous Stratospheric Chemistry.....	8.10
8.3 THE CURRENTLY OBSERVED ATMOSPHERE: 1980–1990.....	8.14
8.3.1 Chlorine and Bromine Loading	8.14
8.3.2 Observed and Calculated Ozone: 1980 baseline	8.14
8.3.3 Modeled Ozone Depletion: 1980 to 1990	8.19
8.4 PREDICTING THE FUTURE ATMOSPHERE: 1990–2050	8.33
8.4.1 Time Lines of Change	8.33
8.4.2 Patterns of Ozone Change	8.36
8.4.3 Peak Chlorine Loading and Integrated Halocarbon Effects	8.41
8.5 OPTIONS AND ISSUES TO 2100	8.46
REFERENCES.....	8.47

FUTURE Cl-Br LOADING AND OZONE DEPLETION

SCIENTIFIC SUMMARY

The atmospheric loading of chlorine and bromine compounds and corresponding predictions of current and future ozone changes are examined using global two-dimensional models of stratospheric chemistry and transport. There has been a major advance in the two-dimensional assessment models used here: most models now include currently-known heterogeneous chemical reactions on the stratospheric sulfate layer. Further, three models also incorporate a parametric formulation of the chemistry involving polar stratospheric clouds (PSCs), but PSC simulations remain incomplete. Results are shown from these three types of models, denoted GAS (gas phase chemistry only), HET (includes reactions of N_2O_5 and $ClONO_2$ on sulfate-layer aerosols), and PSC (includes parameterization of PSC-chemistry). The HET models predict a substantially different balance among the chlorine, bromine, odd-hydrogen, and odd-nitrogen cycles for ozone destruction in the lower, mid-latitude stratosphere than do the GAS models, with important implications for the ozone response to a variety of perturbations in trace gases (*e.g.*, chlorofluorocarbons (CFCs), halons, methane, nitrous oxide, and nitric oxides from aircraft). The only forcing considered in the model scenarios is the evolving atmospheric composition, which over the past decade has been dominated by the increase in halocarbon chlorine loading from 2.5 to 3.6 ppbv.

GAS models predict integrated column depletions and vertical profiles of ozone loss from 1980 to 1990 that are much less than those observed at middle latitudes over all seasons in both hemispheres.

HET models simulate most of the observed column ozone loss from 1980 to 1990 for the northern middle latitudes in summer, but only about half of that in winter (see Table 8-A below). Unlike previous assessments, the predicted vertical profile of ozone loss from 1980 to 1990 has the same structure as observed, including substantial losses in the lower middle latitude stratosphere. Largest relative ozone losses at 45°N from 1980 to 1990 are predicted to range from 7 percent to 16 percent near 44-km altitude, and, compared with observations, are similar in shape (loss versus altitude) but greater in magnitude. The sensitivity of these results to substantial (factor of 4) changes in the sulfate layer area is small (about 1/2 percent change in column ozone over the past decade). Similar results hold for the Southern Hemisphere, except near 60°S in winter-spring, where observed losses greatly exceed those predicted.

PSC models are still under development; current versions predict greater ozone loss at northern middle latitudes in winter.

Table 8-A Approximate Ranges of Column Ozone Losses (percent) for 1980-1990

lat./months	TOMS*		GAS		HET		PSC	
	JFM	JAS	JFM	JAS	JFM	JAS	JFM	JAS
60°N	6-8	3-4	1-2	1	3-4	3	5-7	3-4
30°N	4-5	1-2	1	<1	2-3	1-2	2	1-2

*TOMS (Total Ozone Mapping Spectrometer) from Figure 2-11.

We expect that atmospheric loading of chlorine and bromine will peak in the late 1990s at levels of about 4.1 ppbv and 25 pptv, respectively. The HET models predict the maximum ozone loss circa 2000, with the additional losses for the period 1990-2000, will be equal to or slightly less than those for 1980-1990. Predictions for the year 2050 depend on many competing changes in Cl_y , Br_y , NO_y (through nitrous oxide), CH_4 , and stratospheric temperatures (through CO_2 and O_3 changes), and thus the model predictions show large differences.

FUTURE Cl-Br LOADING AND OZONE DEPLETION

The peak chlorine loading in the late 1990s may vary over a range of 0.2 ppbv in response to a wide variety of options for halocarbon phaseouts and hydrochlorofluorocarbon (HCFC) substitution. A significant reduction in peak chlorine loading can be achieved with accelerated phase-out schedules of CFCs, carbon tetrachloride, and methyl chloroform. The times at which chlorine loading falls below 3 and 2 ppbv can be shifted by at most 10 years with such an acceleration of the phaseout. The integral of high chlorine levels (*i.e.*, cumulative exposure to ozone loss and, hence, ultraviolet (UV) increases) is more sensitive to the differences between certain policy options: heavy substitution with HCFCs can increase this number by at most 20 percent, whereas accelerated phaseouts can reduce it by as much as 50 percent. Acceleration of the halon phaseout by 3 years would reduce peak bromine loading by 1 pptv (about 4 percent). Stringent controls on current use of HCFC-22, or on substitution with alternative HCFCs, would not significantly reduce peak chlorine, but would accelerate the decay in chlorine loading in the decades following the peak. Scenarios in Table 8-B show the sensitivity of tropospheric chlorine loading to a range of halocarbon phase-out schedules.

To represent the differences in effectiveness of halocarbons in destroying ozone, we define a new quantity: the stratospheric free halogen content (FH in ppbv), the weighted sum of the free chlorine (FC in ppbv), and free bromine (FB) in the stratosphere, which are measures of the Cl_y and Br_y , respectively, available in the stratosphere to contribute to ozone depletion (*e.g.*, particularly in the lower, high-latitude stratosphere). The FC is calculated from the chlorine loading by weighting individual chlorocarbons by a factor proportional to their relative ozone depletion potentials (ODPs). All of the bromine in the halons and methyl bromide is assumed to be available in the stratosphere as Br_y , which is 30 to 120 times more effective per atom than Cl_y in catalyzing ozone loss (*i.e.*, the scale factor to convert FB into the same units as FC and FH, effective ppbv of Cl_y). These preliminary calculations of FH demonstrate that a large proportion (0.8 to 2.8 ppbv) is due to bromine, predominantly methyl bromide. But, the Br_y/Cl_y scale factor is highly uncertain due to large uncertainties in the bromine chemistry and to differences in the model calculations of Br_y -catalyzed ozone destruction.

FUTURE Cl-Br LOADING AND OZONE DEPLETION

Table 8-B Scenarios for Reducing Chlorine and Bromine Emissions

Case	Peak (ppbv Cl _y)			Year when		Integral > 1985 Value (ppbv-year)		
	CL	FC	FH	CL<3	CL<2	CL	FC	FH
AA	4.11	3.24	4.17	2027	2061	22.8	12.6	16.8
AA/X	-0.18	-0.12	-0.14	-10	-7	-33%	-28%	-24%
D	-0.03	-0.04	-0.04	0	0	-6%	-9%	-7%
D/X	-0.10	-0.07	-0.09	0	0	-13%	-21%	-16%
E	0.00	0.00	0.00	-7	-3	-8%	-1%	-1%
E/X	-0.03	-0.01	-0.01	-10	-3	-18%	-6%	-5%
AA+D/X	-0.21	-0.13	-0.16	-11	-7	-45%	-46%	-39%
AA+D+E/X	-0.21	-0.13	-0.16	-18	-13	-53%	-48%	-41%
AA+HH/X	-0.18	-0.12	-0.17	-10	-7	-33%	-28%	-29%
XX	-0.21	-0.13	-0.18	-22	-19	-64%	-59%	-59%
F20	+0.01	0.00	0.00	+1	0	+3%	+3%	+3%
F40	+0.02	0.00	0.00	+1	0	+6%	+6%	+5%
G20	+0.01	0.00	0.00	+5	+2	+18%	+15%	+14%

CL = Chlorine loading (in ppbv) is the sum of the mean tropospheric mixing ratio of chlorine in the form of chlorocarbons. The 1985 value for CL is 3.00 ppbv.

FC = Free chlorine in the lower stratosphere is the weighted sum of the chlorocarbons (CFC-11 × 2.70, CFC-12 × 1.08, CFC-113 × 1.8, CFC-114 × 1.16, CFC-115 × 0.12, CCl₄ × 3.80, CH₃CCl₃ × 2.94, CH₃Cl × 0.99, HCFC-22 × 0.32, HCFC-A/B × 0.99). The 1985 value for FC is 2.45 ppbv.

FH = Free halogen in the lower stratosphere is equal to FC plus 40 times the bromocarbon concentrations (halons 1211 and 1301, CH₃Br). The 1985 value for FH is 3.18 ppbv.

Scenario AA: Protocol (10-year lag of 10 percent of CFCs and CCl₄, no lag for CH₃CCl₃ and halons. HCFC-22 (+3 percent/year 1991 → 2020, ramps to 0 by 2040), No other HCFCs.

Other Scenarios (all relative to AA):

AA/X: CFC and CCl₄ schedules accelerated 3 years, (1994+ → 1991+)

HH/X: Halon schedule accelerated 3 years (1994+ → 1991+)

D: CH₃CCl₃ schedule accelerated 3 years

D/X: CH₃CCl₃ phaseout on accelerated CFC schedule (1993+ only)

E: HCFC-22 ramp to 0 from 2000 to 2020

E/X: HCFC-22 phaseout on accelerated CFC schedule (1993+ only)

XX: CUT ALL halocarbon emissions in 1993.

Substitution with HCFCs begin in 1995 (percent of 1985 CFC prod.), +3 percent/year to 2020, ramp to 0 by 2030:

F20: 20 percent substitution with HCFC-A (molecular weight 135, 1 Cl, 2-year lifetime)

F40: 40 percent substitution with HCFC-A

G20: 20 percent substitution with HCFC-B (molecular weight 135, 1 Cl, 20-year lifetime)

8.1 INTRODUCTION

The prediction of future ozone requires three elements: (1) a scenario for the net emissions of chemically and radiatively active trace gases from the land and oceans; (2) a global atmospheric model that projects the accumulation of these gases; and (3) a chemical transport model that describes the distribution of ozone for a prescribed atmospheric composition and climate. This chapter, of necessity, presents models for all three elements and focuses on the: (1) atmospheric abundance of chlorine and bromine in the form of halocarbons; and (2) the associated perturbations to stratospheric ozone.

Primary emissions of the trace gases are the cornerstone of any model of atmospheric composition. We are concerned only with those gases that are transported readily into the stratosphere and that play important roles in the chemical or dynamical processes there. This chapter deals primarily with chlorine and bromine whose atmospheric abundances are dominated by known industrial sources. Scenarios for the future emissions of currently used halocarbons (CFCl_3 , CF_2Cl_2 , $\text{CF}_2\text{ClCFCl}_2$, $\text{CF}_2\text{ClCF}_2\text{Cl}$, $\text{CF}_3\text{CF}_2\text{Cl}$, CCl_4 , CH_3CCl_3 , CHF_2Cl , CF_2ClBr , CF_3Br) and possible chlorine-containing substitutes (CF_3CHCl_2 , CF_3CHFCl , CH_3CFCl_2 , $\text{CH}_3\text{CF}_2\text{Cl}$) are based on the current Montreal Protocol (1987, revised 1990, London) and on simple assumptions about future regulations and market growth. Other halocarbons (CH_3Cl , CH_3Br) are held fixed. No attempt is made to derive emissions scenarios for the other important trace gases (CO_2 , N_2O , CH_4) for which concentrations are extrapolated into the next century using current trends.

The atmospheric concentrations of trace gases may be predicted from the net emissions using an atmospheric model describing both transport and the chemical-physical losses. The scientific community has developed two- and three-dimensional chemical transport models for the purposes of interpreting observations or defining sources and sinks of all the major trace gases. Here we must simplify our treatment of atmospheric composition by compressing the detailed, multidimensional chemical losses into a single, bulk atmospheric lifetime (e-folding time). For species that are not predominantly of industrial origin, we adopt an even simpler approach of specifying future abundances based on

current trends. For the past two decades, we can define the bulk tropospheric (average) composition from observations.

Stratospheric ozone is the focus of this assessment, and this chapter reports predictions of ozone changes using the best global two-dimensional models of stratospheric chemistry and transport currently in use within the international scientific community. These models are not three-dimensional and thus cannot include the full range of dynamical coupling, *e.g.*, between the large Antarctic ozone losses and the circulation itself. Results presented here are, however, a significant step beyond those reported in previous United Nations Environment Program-World Meteorological Organization (UNEP-WMO) assessments (WMO, 1990a; 1990b). The models now incorporate heterogeneous chemical reactions expected to occur on the ubiquitous stratospheric sulfate layer, and some models have included a parametric formulation of the chemistry involving PSCs. Calculations are shown for the past decade and into the next century. We examine not only perturbations to column ozone (and hence solar ultraviolet at the ground), but also changes in local ozone concentrations and in key species that drive stratospheric chemistry.

8.2 ATMOSPHERIC COMPOSITION AND CHEMISTRY

In this assessment, the stratospheric ozone models are forced by specifying the composition of the bulk troposphere from 1970 through 2050. Observations are used for the period 1970-1990. After 1990, we adopt a single projection for those species unaffected by the Montreal Protocol and its revisions, but examine a range of options for those halocarbons likely to fall under regulation.

The lower troposphere in these scenarios is treated as a single, well-mixed box (of uniform composition) that acts as a lower boundary condition for the chemical transport models. This assumption is reasonable for the time scales considered here, but ignores the well-defined latitudinal gradients and other spatial variations in trace gas concentrations throughout the lower atmosphere. The troposphere mixes vertically and within hemispheres on time scales of a few months (*e.g.*, Mahlman *et al.*, 1980); interhemispheric transport is slower, taking about a

FUTURE CI-Br LOADING AND OZONE DEPLETION

year (e.g., Cunnold *et al.*, 1986). The observed and expected interhemispheric gradients in the important trace gases are small (less than 10 percent with the exception of CH_3Br , see Chapter 1) and are not expected to induce significant hemispheric asymmetries in the stratosphere.

Transport of trace gases from the troposphere to the stratosphere is predicted to take as long as 5 years depending upon where in the stratosphere and which model (see Jackman *et al.*, 1989a). This time lag in stratospheric response to tropospheric forcing is simulated automatically by the stratospheric models used here when the calculations are performed in a time-dependent manner (*i.e.*, the lower boundary conditions are reset annually according to the scenario). In this case, the model simulation must continuously calculate every year in the scenario, from the initialization (1970) to the final year (2050). (Results from the different models for the initial year, 1970, are not easily compared because they depend so much on the individual initializations of each model, rather than on the universally adopted boundary conditions from the scenario.) When models are used to study a specific year, the calculation is often done as a steady-state atmosphere (*i.e.*, periodically repeating annual cycle with the same fixed boundary conditions). For these stratosphere models, we have chosen steady-state boundary conditions corresponding to the time-dependent scenario of 2.5 years previous in order to approximate the time lag in stratospheric transport (Holton, 1990). The true delay will be shorter than 2 years in the lower stratosphere, and may be longer at high altitudes and within the wintertime polar vortex (Schmidt and Khedim, 1991).

This section summarizes the scenario model for trace gas composition (all mixing ratios are vol/vol), including the lifetimes of the halocarbons, the historical record, the options for control of future halocarbon abundances, and the assumed stratospheric chemical model.

8.2.1 Lifetimes of the Halocarbons

The lifetimes of those gases with only stratospheric destruction (*i.e.*, the chlorofluorocarbons, carbon tetrachloride, Halon-1301, and nitrous oxide) should, in principle, be calculated directly from the global stratospheric chemical

transport models. The model-derived lifetimes for these gases are in basic agreement, but no better than ± 20 percent. The range of calculated lifetimes for the principal halocarbons are presented in Table 8-1. The empirically derived lifetimes from a budget analysis of the Atmospheric Lifetime Experiment-Global Atmospheric Gases Experiment (ALE-GAGE) observations (Cunnold *et al.*, 1986) provides no further constraint.

For this assessment, we have had to agree on a single set of lifetimes for the halocarbons. A midrange value of 55 years was selected for CFCl_3 . The other stratospheric lifetimes (with the exception of Halon-1211) were scaled to the 55-year lifetime for CFCl_3 by noting that for most models the ratios of lifetimes for the CFCs were in better agreement than their absolute values. The relative lifetimes for different CFCs within a model are believed to be mainly independent of the specific circulation. The circulation patterns vary substantially from model to model (see Jackman *et al.*, 1989a) and are believed to be the cause of the large range in CFC lifetimes reported in Table 8-1. Nevertheless, this assumption is too simple. For example, the CFCl_3 lifetime is sensitive to transport below 25 km whereas the CF_2Cl_2 lifetime is determined by the transport to altitudes above 25 km, and transport in these different regimes does not scale similarly in all models.

Several currently important halocarbons (CH_3CCl_3 , CHF_2Cl) and all proposed substitutes (the HCFCs) are destroyed in the troposphere by reaction with OH. Losses in the lower atmosphere dominate; stratospheric destruction is minor, see Table 8-2. Tropospheric chemistry models for the global distribution of OH have significant uncertainties, about ± 30 percent (see AFEAS, 1990; WMO, 1990). These chemistry models can be based on the observed climatologies of important species such as O_3 , $\text{NO} + \text{NO}_2$, H_2O , CO , and sunlight (Spivakovsky *et al.*, 1990) or they can be calibrated against other trace species that react primarily with OH such as ^{14}CO (Derwent and Volz-Thomas, 1990) or CH_3CCl_3 (Prinn *et al.*, 1987). Considering the estimates of tropospheric OH from a combination of such models, we have arbitrarily chosen a tropospheric OH distribution that corresponds to a CH_3CCl_3 lifetime of exactly 7 years with respect to reaction with OH in the troposphere. (A unique mean OH concentration cannot be derived from this assumption.) Based on

FUTURE CI-Br LOADING AND OZONE DEPLETION

Table 8-1 Stratospheric Lifetimes and Halocarbons Scenarios

Species	Abbreviation	Lifetime (yr)	Lifetime (range)	Emissions (kt/year)	Factor (kt/pptv)
CFCl ₃	F11	55	(42-66)	360	23.2
CF ₂ Cl ₂	F12	116	(57-105) ^{A/G} (95-130) (67-333) ^{A/G}	450	20.4
CF ₂ ClCFCl ₂	F113	110	(75-144)	165	31.6
CF ₂ ClCF ₂ Cl	F114	220	(197-264)	15	28.9
CF ₃ CF ₂ Cl	F115	550	(400-800)	10	26.1
CCl ₄	CTC	47	(30-58)	80	25.9
CF ₂ ClBr	1211	11	(10-20)	10	27.9
CF ₃ Br	1301	77	(69-88)	9	25.1
CF ₂ BrCF ₂ Br	2402	20*	(22-30)		
N ₂ O		132*	(110-168)		
CH ₃ CCl ₃	MCF	6.1	(5.1-6.4) ^{A/G}	600	22.4
CHF ₂ Cl	H22	15.8		140	14.6
C _x H _y F _x Cl	HX	20		(tbd)	22.
C _x H _y F _x Cl ₂	HY	2		(tbd)	22.

Note: A/G = ALE/GAGE. The quoted range in lifetimes refers to calculations by the participating models, including those used in Chapter 6; lifetimes derived empirically from a budget analysis of the ALE/GAGE data (Cunnold *et al.*, 1986; Prinn *et al.*, 1992) are noted. The short lifetime for Halon 1211 is due to photolysis in the upper tropical troposphere. The quoted lifetimes(*) for Halon 2402 and N₂O are not used in these scenarios but are needed for ODP and GWP calculations. For the lifetimes of CH₃CCl₃ and CHF₂Cl, see Table 8-2 Lifetimes for Tropospheric Loss. The base level of emissions assumed for 1985 are given. Factor is the global budget relationship of species mass (kilotons) per tropospheric average mixing ratio (pptv). The properties of the two surrogate substitutes, HX and HY, are also given. Here and throughout this document, the notation for mixing ratio (pptv = 10⁻¹², ppbv = 10⁻⁹, ppmv = 10⁻⁶) refer to number density (vol/vol). Emissions refer to the 1985 baseline levels.

the analysis of Prather and Spivakovsky (1990), the tropospheric lifetimes of other trace gases that react with OH can be accurately calculated by scaling the ratio of their respective rate coefficients evaluated at a temperature of 277 K. The contribution of stratospheric losses are added on (inverse sum), and the net atmospheric lifetimes are given in Table 8-2. The resulting lifetime for CH₃CCl₃ is in excellent agreement with the most recent ALE/GAGE analysis (Prinn *et al.*, 1992). If recalibration of the CH₃CCl₃ data from ALE/GAGE reduces concentrations by 10 percent (see Chapter 1), then it is likely that analyses (currently underway) may recommend a shorter lifetime and hence greater tropospheric OH levels.

It must be recognized that the mean atmospheric residence time describing the decay rate of a specific halocarbon, denoted here simply as the lifetime, is inherently a variable quantity. Stratospheric losses

may change in a future atmosphere with a different circulation and ozone columns. Similarly, we may expect that the lifetimes of the HCFCs would change as tropospheric OH responds to the overall global changes in composition and climate.

An international scientific working group is currently reexamining the CFC and HCFC atmospheric lifetimes, focusing on both *ab initio* model calculations and empirical analyses of global budgets. Results from this study will be available in early 1992 and may lead to a revision in the lifetimes adopted here.

8.2.2 Historical Record and Projections

The important non-halocarbon species for stratospheric modeling are N₂O, CH₄ and CO₂. Nitrous oxide is the primary stratospheric source of

FUTURE Cl-Br LOADING AND OZONE DEPLETION

Table 8-2 Lifetimes for Tropospheric Loss

Species	Abbreviation	k (OH + Species)		τ trop	Lifetimes (year)	
		A	B		τ strat	τ Net*
CH ₃ CCl ₃	MCF	5.0E-12	1800	7.00	47	6.1
CHF ₂ Cl	H22	1.2E-12	1650	17.0	240	15.8
CH ₂ F ₂	H32	2.8E-12	1650	7.3	infinite	7.3
CF ₃ CHCl ₂	H123	6.4E-13	850	1.77	47	1.71
CF ₃ CHFCl	H124	6.6E-13	1250	7.28	129	6.9
CHF ₂ CF ₃	H125	6.0E-13	1700	40.7	infinite	40.7
CF ₃ CH ₂ F	H134a	1.3E-12	1650	15.7	infinite	15.7
CH ₃ CFCl ₂	H141b	9.4E-13	1500	12.6	76	10.8
CH ₃ CF ₂ Cl	H142b	1.4E-12	1800	25.0	215	22.4
CH ₃ CF ₃	H143a	1.6E-12	2100	64.6	infinite	64.6
CH ₃ CHF ₂	H152a	1.3E-12	1050	1.80	infinite	1.80
CF ₃ CF ₂ CHCl ₂	H225ca	2.0E-12	1300	2.88	120*	2.81
CF ₂ ClCF ₂ CHClF	H225cb	6.7E-13	1300	8.59	120*	8.0
CH ₄	methane	3.9E-12	1885	12.2	147	11.3
C ₂ H ₆	ethane	1.1E-11	1100	0.25	50	0.25
C ₃ H ₈	propane	1.4E-11	750	0.06	50	0.06
CH ₃ Cl	methyl chloride	2.1E-12	1150	1.59	50	1.54
CH ₃ Br	methyl bromide	6.8E-13	850	1.67	50	1.62
CH ₂ Cl ₂	methylene chloride	5.8E-12	1100	0.48		0.48
C ₂ Cl ₄	perchlor-ethylene	9.4E-12	1200	0.43		0.43
C ₂ HCl ₃	trichlor-ethylene	4.9E-13	-450	0.021		0.021

Note: The notation H is an abbreviation for hydrochlorofluorocarbon (HCFC). The rate coefficients for reaction with OH, $k = A \exp(-B/T(K)) \text{ cm}^3\text{s}^{-1}$, are taken from the most recent reviews (JPL-90, IUPAC-91, see Chapter 3). We assume a global tropospheric OH corresponding to a CH₃CCl₃ tropospheric lifetime equal to 7 years; the tropospheric lifetimes for other species are scaled by the ratio of the rate coefficients at 277 K (Prather and Spivakovsky, 1990). Stratospheric lifetimes are based on direct or scaled model calculations, except for infinite (assumed no stratospheric loss) and for H225c isomers (120* is an estimate). The Net lifetime is the inverse average of the tropospheric and stratospheric lifetimes. The Net lifetime for CH₃CCl₃ is in agreement with the most recent ALE-GAGE empirical value of 5.1 to 6.4 year, (Prinn *et al.*, 1991). If there were an additional loss process for CH₃CCl₃ such as oceanic hydrolysis, the Net derived lifetime for CH₃CCl₃ alone would be reduced, but still fall within the empirically derived range.

Using current estimates for emissions of CH₂Cl₂ (500 kt/year), C₂Cl₄ (500 kt/year), and C₂HCl₃ (300 kt/year), these gases would contribute 0.035, 0.032, and 0.001 ppbv, respectively, to the tropospheric chlorine loading.

$$*1/\tau_{\text{Net}} = 1/\tau_{\text{Trop}} + 1/\tau_{\text{Strat}}$$

odd-nitrogen compounds (NO_y = NO + NO₂ + NO₃ + 2xN₂O₅ + HNO₃ + HO₂NO₂ + HONO + ClONO₂ + BrONO₂). NO_y-related chemistry is responsible for a large fraction of stratospheric O₃ loss, controls partitioning in the Cl_y family (Cl_y = HCl + ClO + 2xCl₂O₂ + Cl + 2xCl₂ + OClO + HOCl + ClONO₂ + BrCl), and suppresses the odd-hydrogen abundance (HO_x = OH + HO₂ + 2xH₂O₂). Methane plays a direct role in the HO_x chemistry and couples with Cl_y chemistry through the formation of HCl, as well as adding to stratospheric H₂O when oxidized. Carbon dioxide does not participate directly in stratospheric

chemistry, but does affect the radiative balance of both stratosphere and troposphere. Some of the participating stratospheric models include the enhanced cooling and reduced stratospheric temperatures associated with increasing concentrations of CO₂ (and global tropospheric warming).

Observations of N₂O, CH₄ and CO₂ over the past 2 decades reasonably define their global tropospheric abundances (see Chapter 1). Table 8-3 gives the bulk tropospheric concentrations at 5-year intervals from 1970 through 1990; a linear interpolation is assumed for intermediate years. The currently-observed trends

FUTURE Cl-Br LOADING AND OZONE DEPLETION

in N₂O (+0.25 percent/year) and CH₄ (+13 ppbv/year) are continued at the same rate until 2050. Predicting future CH₄ growth is a guessing game, but there seems to be an overall trend to lower growth rates. There is strong evidence that human activities are responsible for these increases, but a satisfactory reconciliation of the sources for these gases is not yet possible. The CO₂ increases (+0.6 percent/year) are based on a fit to the Intergovernmental Panel on Climate Change (IPCC) (1990) business-as-usual (BaU) scenario.

We have assumed that the only natural source of stratospheric chlorine, methyl chloride, remains constant throughout these scenarios at 600 pptv. Nevertheless, we have only limited observational evidence that CH₃Cl has remained constant over the past two decades. Similarly, the abundance of CH₃Br is assumed to remain constant at 15 pptv. Methyl bromide, however, presents a particular problem: it

is used as a grain fumigant with potentially large emissions; the large north-south gradient and high variability in northern mid-latitudes (Penkett *et al.*, 1985) also point to an industrial source; and it is the predominant source of stratospheric bromine in these calculations. Thus, the lack of a good historical record for CH₃Br, or of an understanding of the industrial emissions, introduces significant uncertainty into the bromine-loading scenarios used here.

The adopted abundances of the industrial halocarbons for the period 1970-1990 are given in Table 8-3. Data are not adequate to define tropospheric abundances in the early 1970s, and we have extrapolated backward smoothly, based in some cases on estimates of emissions. The projected concentrations of these halocarbons are calculated from several emission scenarios discussed in the following section, using the lifetimes described above.

Table 8-3 Historical Record (1970-1990) and Projections

Year	CO ₂ (ppmv)	N ₂ O (ppbv)	CH ₄ (ppbv)	CH ₃ Cl (pptv)	CH ₃ Br (pptv)
1970	325	295	1420	600	15
1975	331	298	1495	600	15
1980	337	302	1570	600	15
1985	345	306	1650	600	15
1990	354	310	1715	600	15
1991+	x1.006	x1.0025	+13	fixed	fixed

Year	F11	F12	F113	F114	F115	1211	1301	H22	CTC	MCF
1970	60	120	2	1	0	0.1	0.1	10	85	40
1975	115	205	6	2	1	0.2	0.2	27	90	70
1980	173	295	15	4	2	0.5	0.6	54	95	100
1985	222	382	30	5	4	1.5	1.7	80	100	130
1990	284	485	57	8	6	2.5	3.5	104	106	159
(1990 obs)	263	470	71	20				115	107	155
1991+	Use Scenarios A, B, or C below with data from Table 8-1									

Note: All halocarbons are in pptv.

These scenarios were based on previous assessments (WMO, 1990b; IPCC, 1990) and defined prior to the work in Chapter 1; they have minor differences for the 1990 observed atmosphere shown here as (1990 obs). See Chapter 1 for references. The large difference in CFC-113 is due to a change in the calibration scale of GAGE measurements. The total tropospheric chlorine loading in the year 1990 from this scenario (3.62 ppbv) and observations (3.56 ppbv) are almost equal since the observations also include some minor halocarbons not part of the scenario.

These scenarios do not include any other year-to-year variability that is known to affect ozone (*e.g.*, solar cycle, quasi-biennial oscillation, or volcanoes). For a more detailed analysis of the period 1955-1985, see Chapter 7 of Report of the International Ozone Trends Panel (WMO, 1990a).

FUTURE CI-Br LOADING AND OZONE DEPLETION

8.2.3 Montreal Protocol: Halocarbon Scenarios

The model for future concentrations of the industrially-produced halocarbons is based on three options for future growth and regulation: the baseline reference case (M) attempts to approximate the current Montreal Protocol (1987, revised 1990, London), as summarized in Table 8-4, are implemented globally with no exception; that CHF₂Cl (HCFC-22) is phased out similarly to CH₃CCl₃ (see Table 8-4); and that no additional chlorine-containing halocarbons are produced. This baseline results in a complete phaseout of all halocarbon production by the year 2005. Note that the phaseout of CFCs is expected to begin substantially before the year 2000, and thus peak chlorine loading is almost 1 ppbv below previous expectations (*e.g.*, Figure 4 of Prather and Watson, 1990).

Three variations of this minimum, baseline scenario are chosen for the stratospheric model calculations. They are summarized in Table 8-5. Scenario A assumes near-global compliance with the Protocol but allows for 10 percent of the CFC market to continue without growth until a complete phaseout in the year 2010. Scenario B is similar to A except that the 10 percent of the CFC market grows at a rate of 5 percent/year until the year 2020 (reaching 430 kton/year). Scenario C examines one possibility when the world market replaces CFC use with alternative HCFCs in addition to conservation, not-in-kind use, and HFCs (hydrofluorocarbons). Scenario C follows Scenario A, except that one long-lived HCFC alternative, H_x with a lifetime of 20 years, is assumed to replace about 30 percent of the CFC plus HCFC-22 market beginning in the year 2000 with 360 kton/year. H_x production is assumed to grow at 3 percent/year until the year 2020, whereupon it is replaced with a short-lived HCFC alternative, H_y, with lifetime of 2 years, and allowed to continue growth at 3 percent/year to the year 2050 (1578 kton/year). Scenario C is an attempt to simulate chlorine loadings that might result from global compliance to a CFC phaseout and market-based projections of HCFC uses.

The calculation of halocarbon concentrations follows the simple box-model integration of Prather and Watson (1990) using lifetimes given in Table 8-1 and emission rates equal to the production as defined

in Scenarios A, B, and C above. The assumption that emission equals production can introduce a phase error in the scenarios because some halocarbons are used in products that do not rapidly release the gas to the atmosphere (*e.g.*, hermetic refrigeration, closed-cell foams). This effect needs to be examined with a more complete model of halocarbon use, but should not induce substantial error in the modeling and comparison of scenarios studied here.

The tropospheric trace gas concentrations for Scenarios A, B, and C are given in Tables 8-6a and 8-6b for the time-dependent and steady-state calculations. The chlorine loading (*i.e.*, total tropospheric chlorine mixing ratio in the form of halocarbons) and bromine loading (similarly defined) are shown in Table 8-7.

8.2.4 Gas Phase and Heterogeneous Stratospheric Chemistry

One key to understanding the chemical processes responsible for the Antarctic ozone hole was the recognition that reactions on the surfaces of stratospheric particles (*i.e.*, heterogeneous chemistry) could activate chlorine-catalyzed ozone loss (see Chapters 3 and 4). It has also been noted recently that reactions on the ubiquitous stratospheric sulfate layer may compete with gas phase photochemistry in the lower stratosphere (see discussion in Chapter 3; Hofmann and Solomon, 1989; Rodriguez *et al.*, 1991; Pitari *et al.*, 1991). Unfortunately, such heterogeneous processes, particularly PSCs, are especially difficult to incorporate (in a generally agreed upon manner) into the global stratosphere models used in these assessments. An attempt was made to formulate a simplified, uniform PSC chemistry for the two-dimensional models, but instead some of the models incorporated polar chemistry in their own way (see model references). The basically non-zonal nature of both PSCs and the circulation of the vortex make the incorporation of polar stratospheric chemistry in a two-dimensional formalism an extremely difficult, possibly intractable, problem (see later discussion and Chapter 4).

Heterogeneous chemistry on the sulfate layer, however, can be defined in a straightforward manner as a homogeneous process, and most of the participating modelers agreed to adopt a standard form. The sulfate-layer chemistry is described in

FUTURE Cl-Br LOADING AND OZONE DEPLETION

Table 8-4 Production Factors for Baseline to Approximate the Montreal Protocol

Year	CFCs	CCl ₄	Halons	CH ₃ CCl ₃	CHF ₂ Cl*
1985*	1.00	1.00	1.00	1.00	1.00
1986*	1.05	1.05	1.05	1.05	1.05
1987*	1.10	1.10	1.10	1.10	1.10
1988*	1.15	1.15	1.15	1.15	1.15
1989*	1.20	1.20	1.20	1.20	1.20
1990*	1.25	1.25	1.25	1.25	1.25
1991	1.00	1.00	1.00	1.30	1.00
1992	1.00	1.00	1.00	1.35	1.00
1993	0.80	1.00	1.00	1.00	1.00
1994	0.80	1.00	1.00	1.00	1.00
1995	0.50	0.15	0.50	0.70	1.00
1996	0.50	0.15	0.50	0.70	1.00
1997	0.15	0.15	0.50	0.70	1.00
1998	0.15	0.15	0.50	0.70	1.00
1999	0.15	0.15	0.50	0.70	1.00
2000	0	0	0	0.30	1.00
2001				0.30	1.00
2002				0.30	1.00
2003				0.30	1.00
2004				0.30	1.00
2005				0	0

*Denotes years or species not explicitly part of the current protocol. The Montreal Protocol invokes 1.00 as the upper limit in midyear of 1990. These factors represent upper limits of production by the participating parties; some countries have already reduced production and may phase out some halocarbons earlier than this schedule.

Table 8-5 Basic Halocarbon Scenarios

M = Baseline scenario assumes emissions equal production as defined in Tables 8-1 and 8-4. Assumes global compliance with the Montreal Protocol plus additional phaseout of all other industrial halocarbons. All halocarbon emissions cease in 2005.

Peak CL = 4.08 ppbv ∫ CL (above 3 ppbv) = 17.9 ppbv-year

A = Baseline scenario, but part of CFC-only market (about 10 percent of 1985 CFC production with the same mix of CFCs) is allowed a 20-year delay in compliance. This CFC production of 100 kton/year continues from 1991 to 2010 with no growth. No HCFC substitutes.

Peak CL = 4.13 ppbv ∫ CL (above 3 ppbv) = 20.8 ppbv-year

B = Baseline scenario, but the CFC noncompliance (as in A, 100 kton/year in 1990) grows at 5 percent/year, reaching 430 kton/year in 2020. Phaseout of all CFCs in 2020. No HCFC substitutes.

Peak CL = 4.14 ppbv ∫ CL (above 3 ppbv) = 22.4 ppbv-year

C = Baseline scenario, including limited non-compliance (as in A), but with an aggressive substitution policy including HCFCs. Begin in 2000 with 360 kton/year (about 30 percent of CFC+HCFC-22 market) of the alternate halocarbon H_x (20-year lifetime), allow growth at 3 percent/year, replace in 2020 with short-lived alternate H_y (2-year lifetime), and continue growth at 3 percent/year (1578 kton/year of H_y in 2050).

Peak CL = 4.13 ppbv ∫ CL (above 3 ppbv) = 22.6 ppbv-year

FUTURE CI-Br LOADING AND OZONE DEPLETION

Table 8-6a Trace Gas Scenarios: Time-Dependent

A (without H _x and H _y) and C (including H _x and H _y)												
Year	F11	F12	F113	F114	F115	1211	1301	H22	CCl ₄	MCF	H _x *	H _y *
1985	222	382	30	5	4	1.5	1.7	80	100	130	0	0
1990	284	485	57	8	6	2.5	3.5	104	106	159	0	0
1995	337	577	81	10	8	3.2	5.2	119	111	176	0	0
2000	337	595	87	11	9	2.9	6.0	127	102	141	0	0
2005	315	581	86	11	9	2.0	5.8	134	91	90	77	0
2010	295	567	85	11	9	1.4	5.6	98	82	40	149	0
2015	271	545	81	11	9	0.9	5.3	71	74	17	220	0
2020	247	522	78	11	9	0.6	4.9	52	66	8	291	0
2025	226	500	74	10	9	0.4	4.6	38	60	3	227	59
2030	206	479	71	10	9	0.2	4.3	28	54	1	177	73
2035	188	459	68	10	9	0.1	4.0	20	48	1	138	86
2040	172	439	65	10	8	0.1	3.8	15	43	0	107	99
2045	157	421	62	9	8	0.1	3.6	11	39	0	83	115
2050	143	403	59	9	8	0.0	3.3	8	35	0	65	133

B														
Year	F11	F12	F113	F114	F115	1211	1301	H22	CCl ₄	MCF				
1985	222	382	30	5	4	Same as in A and C								
1990	284	485	57	8	6									
1995	338	578	81	10	8									
2000	340	600	88	11	9									
2005	323	593	89	11	9									
2010	311	592	91	12	9									
2015	305	597	94	12	10									
2020	305	610	99	13	10									
2025	284	593	96	13	10									
2030	260	568	92	12	10									
2035	237	544	88	12	10									
2040	216	521	84	12	10									
2045	198	499	80	12	10									
2050	180	478	77	11	10									

*In the stratospheric models, H_x is treated as one-half molecule of CF₂Cl₂; H_y as one molecule of CF₂Cl₂.

Table 8-6b Trace Gas Scenarios: Steady State

Year	F11	F12	F113	F114	F115	1211	1301	H22	CCl ₄	MCF	CO ₂	N ₂ O	CH ₄	
A Steady State														
'80SS	149	250	11	3	2	0.4	0.4	41	93	85	334	300	1538	
'90SS	253	434	44	7	5	2.0	2.6	92	103	145	350	308	1685	
'00SS	337	586	84	11	9	3.0	5.6	123	106	158	372	316	1815	
'20SS	259	533	79	11	9	0.7	5.1	62	70	12	419	332	2075	
'50SS	150	412	60	9	8	0.0	3.4	9	37	0	501	358	2465	
B Steady State														
'80SS	149	250	11	3	2	0.4	0.4	41	93	85	334	300	1538	
'90SS	253	434	44	7	5	2.0	2.6	92	103	145	350	308	1685	
'00SS	339	589	85	11	9	3.0	5.6	123	106	158	372	316	1815	
'20SS	305	604	97	13	10	0.7	5.1	62	70	12	419	332	2075	
'50SS	189	489	78	11	10	0.1	3.4	9	37	0	501	358	2465	
C Steady State														
	Same as A except						H _x *	H _y *						
'80SS							0	0						
'90SS							0	0						
'00SS							0	0						
'20SS							256	0						
'50SS							74	124						

*In the stratospheric models, H_x is treated as one-half molecule of CF₂Cl₂; H_y as one molecule of CF₂Cl₂.

FUTURE Cl-Br LOADING AND OZONE DEPLETION

Table 8-7 Tropospheric Chlorine and Bromine Loading

Year	Chlorine (ppbv)			Bromine (pptv)
	A	B	C	A-B-C
1985	3.00	3.00	3.00	18.2
1990	3.62	3.62	3.62	21.0
1995	4.13	4.13	4.13	23.4
2000	4.05	4.07	4.05	23.9
2005	3.76	3.82	3.84	22.8
2010	3.45	3.57	3.60	22.0
2015	3.20	3.44	3.42	21.2
2020	2.99	3.41	3.28	20.5
2025	2.82	3.25	3.16	20.0
2030	2.67	3.07	2.99	19.5
2035	2.53	2.91	2.84	19.1
2040	2.41	2.76	2.71	18.9
2045	2.29	2.63	2.61	18.7
2050	2.19	2.51	2.52	18.3

Table 8-8. One key uncertainty in the formulation is the surface area of sulfate aerosols (see Chapter 3). We gave upper and lower limits for the surface area: the lower limit corresponds to baseline, clean conditions (*i.e.*, several years after any significant volcanic injection of sulfur), and the upper limit, a factor of four greater, is approximately the median value over the past two decades (*i.e.*, about half of the time the surface area exceeded the upper limit). For example, the sulfate layer's optical depth (closely related to surface area) has increased by factors of 20 or more during the past decade following the eruption of El Chichón, (see Figure 3-2). The stratospheric model calculations of the trace gas scenarios included both a gas phase only chemistry using JPL-90

Table 8-8 Heterogeneous Chemistry on the Sulfate Layer Aerosol Surface Area ($10^{-8} \text{ cm}^2\text{cm}^{-3}$)

z*	Jan-Feb-Mar-Apr-May-Jun					Jul-Aug-Sep-Oct-Nov-Dec				
	60-90N	30-60N	30N-30S	30-60S	60-90S	60-90N	30-60N	30N-30S	30-60S	60-90S
	Enhanced (Median)									
32	0.1	0.1	0.4	0.2	0.1	0.1	0.1	0.4	0.3	0.1
30	0.2	0.3	0.7	0.4	0.2	0.2	0.3	0.7	0.6	0.2
28	0.5	0.7	1.3	0.8	0.5	0.5	0.7	1.3	1.0	0.5
26	1.0	1.0	1.7	1.2	1.0	1.0	1.0	1.7	1.5	1.0
24	1.4	1.5	2.0	1.7	1.4	1.4	1.5	2.0	2.0	1.4
22	1.8	2.0	2.5	2.5	2.0	1.8	2.0	2.5	2.5	2.0
20	2.5	2.5	3.0	3.2	3.0	2.5	2.5	3.0	3.0	2.5
18	3.0	3.0	3.0	4.0	4.0	3.0	3.0	3.0	4.0	4.0
16	3.5	3.5	2.0	4.0	4.5	3.0	3.0	2.0	4.0	5.0
14	4.5	4.5	2.0	4.0	5.0	3.5	3.5	2.0	5.0	6.0
12	5.0	5.0	2.0	4.0	5.0	4.0	4.0	2.0	5.0	7.0

Baseline (Lower Limit)

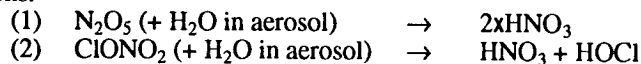
32

.....Divide All Numbers by Four

12

Note: Surface areas based on analysis of SAGE II data by Poole, Thomason, and Yue, see Chapter 3.

Reactions:



Probabilities:

$G_1 = 0.1$
 $G_2 = 0.006 \exp[-0.15 \times (T - 200)]$

where G is the probability of reaction per collision. G_2 depends on the water content of the sulfuric acid. This formula has been fitted to the laboratory data of Tolbert *et al.* (1988) under stratospheric conditions.

Rates:

$k = 5200 \text{ cm/s} \times G \times \text{Surface-Area (/cm)}$

where 5200 cm/s is an effective collision velocity.

FUTURE CI-Br LOADING AND OZONE DEPLETION

kinetics (DeMore *et al.*, 1990) with updates noted in Table 8-2 (denoted GAS), and a sulfate chemistry using the same gas phase kinetics plus the specifications in Table 8-8 (denoted HET for the lower limit of sulfate aerosol areas and HET-E for the enhanced levels of sulfate aerosols).

8.3 THE CURRENTLY OBSERVED ATMOSPHERE: 1980-1990

This section examines the model simulations of stratospheric ozone concentrations for the current epoch. We focus on the period 1980-1990 for which we have the most extensive global observations of ozone from satellites (see Chapter 2). The change in ozone over the past decade is predicted by the participating two-dimensional stratospheric models using different chemical formulations. The models and their chemistries are summarized in Tables 8-9a and b.

Ozone loss prior to 1980 is not discussed here; the choice of 1970 as the initial atmosphere precluded such comparisons. A best estimate of the predicted perturbations prior to 1980 would be that they are comparable to those reported here for the period 1980 to 1990 (*i.e.*, the predicted ozone loss from 1960 to 1990 would be larger, possibly twice as large as that shown here for 1980-1990, but would require additional studies to quantify). There is evidence from the long-term record at Dobson sites (see Chapter 2) that ozone depletion in the 1980s was significantly greater than that in the 1970s. The existence of a high threshold for chlorine levels, above 15 ppbv at which there would be rapidly nonlinear ozone loss (Prather *et al.*, 1984), may need to be reexamined in light of the impact of heterogeneous chemistry on the coupling of the NO_x and Cl_x families in the lower stratosphere.

These scenarios do not include any year-to-year variability that is known to affect ozone (*e.g.*, solar cycle, quasi-biennial oscillation, and volcanoes). For a more detailed analysis of the period 1955-1985, see Chapter 7 of *Report of the International Ozone Trends Panel* (WMO, 1990a). Comparison of these model calculations (which do not include a solar cycle) with observations for the decade 1980-1990 is appropriate because it began and ended near the maximum of the solar cycle.

8.3.1 Chlorine and Bromine Loading

The atmospheric composition has evolved steadily since 1980 (see Chapter 1). As summarized in Table 8-3, CO₂ has increased by about 5 percent, N₂O by 2.5 percent, and CH₄ by about 9 percent. These relative changes are dwarfed by the large increases in halocarbons, leading to a growth in the atmospheric chlorine loading from 1.5 ppbv in 1970 to 2.5 ppbv in 1980 to 3.6 ppbv today. Bromine loading before the year 1980 would have been dominated by natural sources and industrial CH₃Br; but by 1990 the halons contribute about 40 percent to stratospheric bromine.

In the models, ozone perturbations over this period are due, first, to chlorine nearly doubling and, second, to CH₄ and bromine increases. The observed trend over this period cannot be used to calibrate the chlorine-induced ozone depletion calculated by the models without a more exhaustive search to rule out other causes not included in these calculations. For example, we do not include directly any observed temperature trends or climatic "red noise" over this period that might induce changes in stratospheric circulation (see Chapter 2). Likewise, we have neglected other changing influences due to human activity (*e.g.*, aircraft exhaust, combustion by-products, hydrocarbons). The systematic decrease in stratospheric temperatures over these 20 years (-2 K near the stratopause, much less in the lower stratosphere except near the Antarctic ozone hole) is predicted to be primarily a product of O₃ depletion rather than CO₂ cooling and is included in some of the models.

8.3.2 Observed and Calculated Ozone: 1980 Baseline

The column abundance of ozone (1 Dobson Unit = 2.687×10^{16} ozone molecules cm⁻²) is often displayed as a traditional Dobson map showing contours of zonally-averaged column O₃ as a function of latitude and month. The ozone columns calculated by the participating models for the year 1980 are shown in Figure 8-1. Also in Figure 8-1 we present the observations from the Total Ozone Mapping Spectrometer (TOMS) averaged over the years 1979 and 1980. Most models show the same basic pattern as the observed column ozone. The Northern

FUTURE Cl-Br LOADING AND OZONE DEPLETION

Table 8-9a Participating Two-Dimensional Stratospheric Chemistry Models

Group	Investigators/References	Location /References
AER	Malcolm Ko Debra Weisenstein Jose Rodriguez Nien Dak Sze	Atmospheric and Environmental Research, U.S. Ko <i>et al.</i> (1984, 1985, 1989)
DuPont	Don Fisher	DuPont, USA
GSFC	Charles Jackman Anne Douglass	NASA Goddard Space Flight Center, U.S. Douglass <i>et al.</i> (1989), Jackman <i>et al.</i> (1989b, 1990)
ITALY	Guido Visconti Giovanni Pitari Eva Mancini	University of Aquila, Italy Pitari and Visconti (1985, 1991), Pitari <i>et al.</i> (1991)
JMRI	Toru Sasaki	Meteorological Research Institute, Japan
LLNL	Don Wuebbles Peter Connell Doug Kinnison	Lawrence Livermore National Laboratory, U.S.
MPI	Christoph Bruehl Paul Crutzen	Max Planck Institute for Chemistry, Germany Bruehl and Crutzen (1988)
NCAR	Guy Brasseur Claire Granier	National Center for Atmospheric Research, U.S.
NOCAR	Susan Solomon Rolando Garcia	NOAA Aeronomy Lab, U.S. NCAR, U.S.
Oslo	Ivar Isaksen Björg Rognerud Frode Stordal	University of Oslo, Norway Stordal <i>et al.</i> (1985), Isaksen <i>et al.</i> (1990) NILU, Norway
SPB	Sergey Zvenigorodsky Sergey Smyshlayev	Environ. Branch, St. Petersburg, Russia Krecov and Zvenigorodsky (1990)

Table 8-9b Chemical Model Calculations

Group	Chemical Models
AER	GAS TD, GAS SS, HET/E SS
GSFC	GAS TD, HET TD, HET/E TD
ITALY	GAS SS, HET SS, HET/E+PSC SS
JMRI	GAS SS
LLNL	GAS SS, HET SS, HET/E SS
MPI	GAS TD
NCAR	GAS SS, HET SS, HET/E SS, HET/E+PSC SS
NOCAR	GAS SS, HET SS
Oslo	GAS TD, HET/E+PSC TD
SPB	GAS TD, GAS SS

Note: The GAS and HET chemical formulations are described in section 8.2.4. Some models simulate enhanced polar ozone loss through PSC-type processing (+PSC). The HET chemistry includes both lower limits (baseline) and higher levels (enhanced or /E) of sulfate surface area, see Table 8-8. The term SS refers to steady state (*i.e.*, single-year run); TD, to time-dependent (*i.e.*, full 70-year) scenario. The NOCAR model (lower boundary at 100 mbar) does not calculate O₃ columns.

FUTURE Cl-Br LOADING AND OZONE DEPLETION

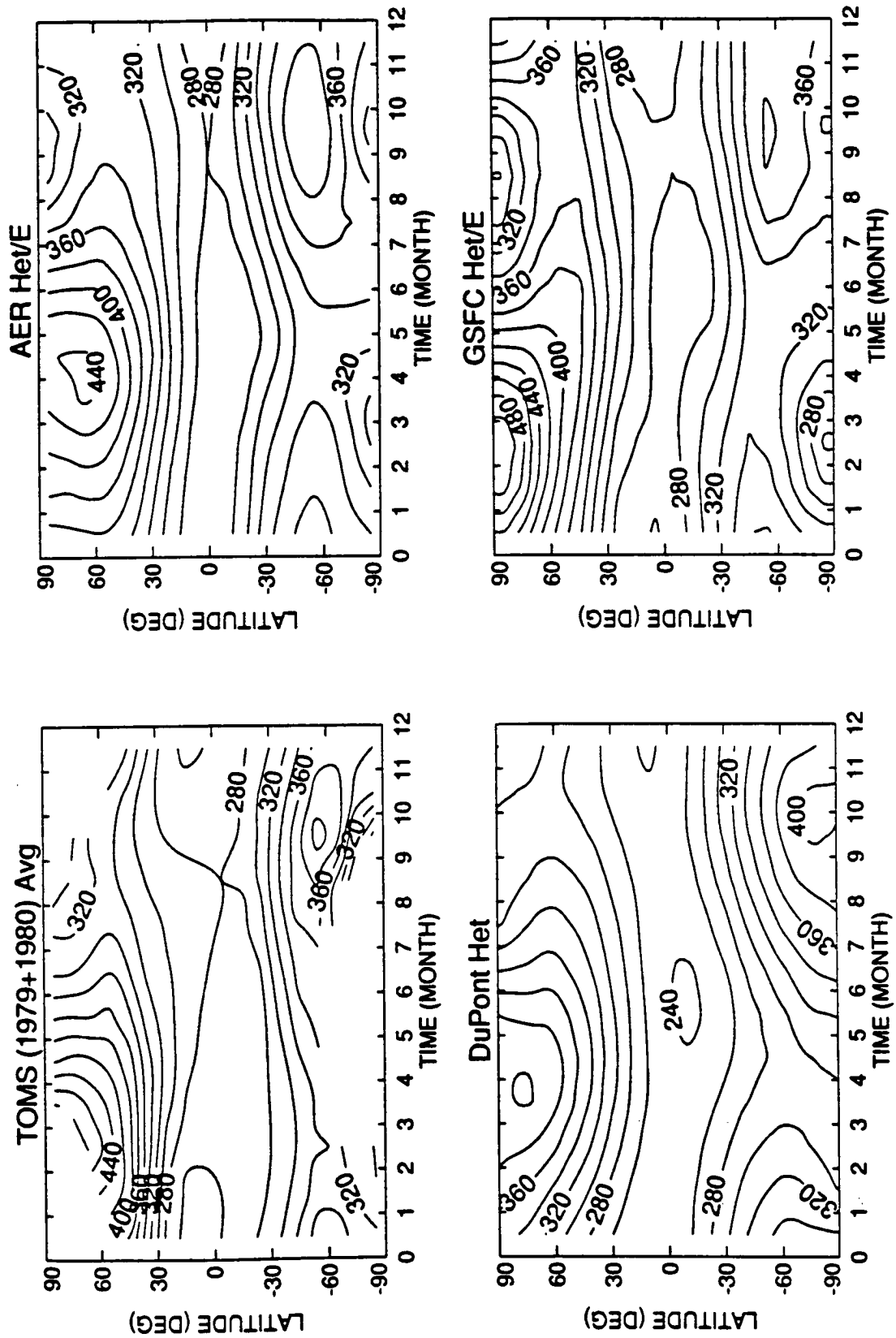


Figure 8-1a Column ozone abundances (Dobson Units) circa 1980 from observations (TOMS) and models.

FUTURE CI-Br LOADING AND OZONE DEPLETION

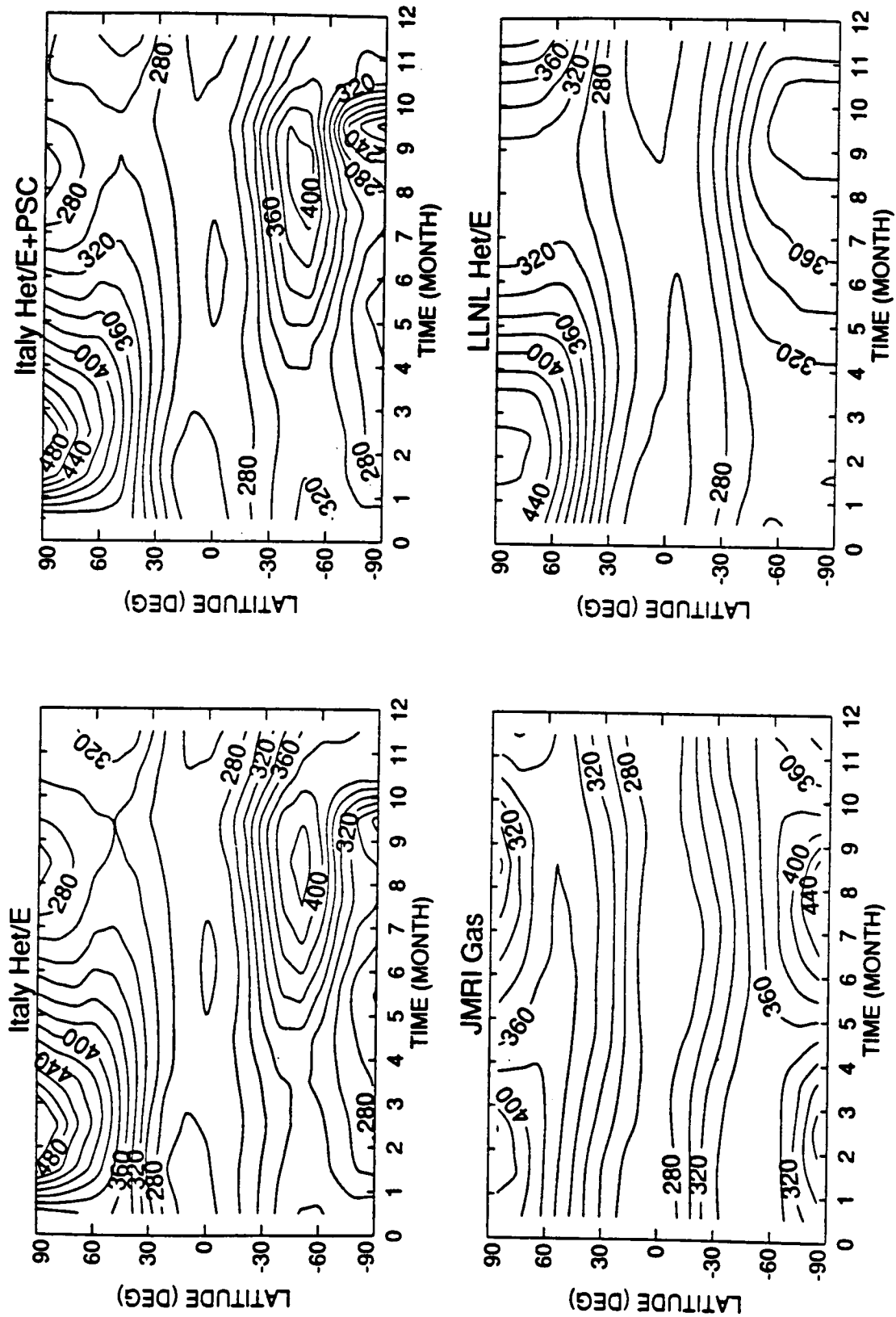


Figure 8-1b Column ozone abundances (Dobson Units) circa 1980 from observations (TOMS) and models.

FUTURE Cl-Br LOADING AND OZONE DEPLETION

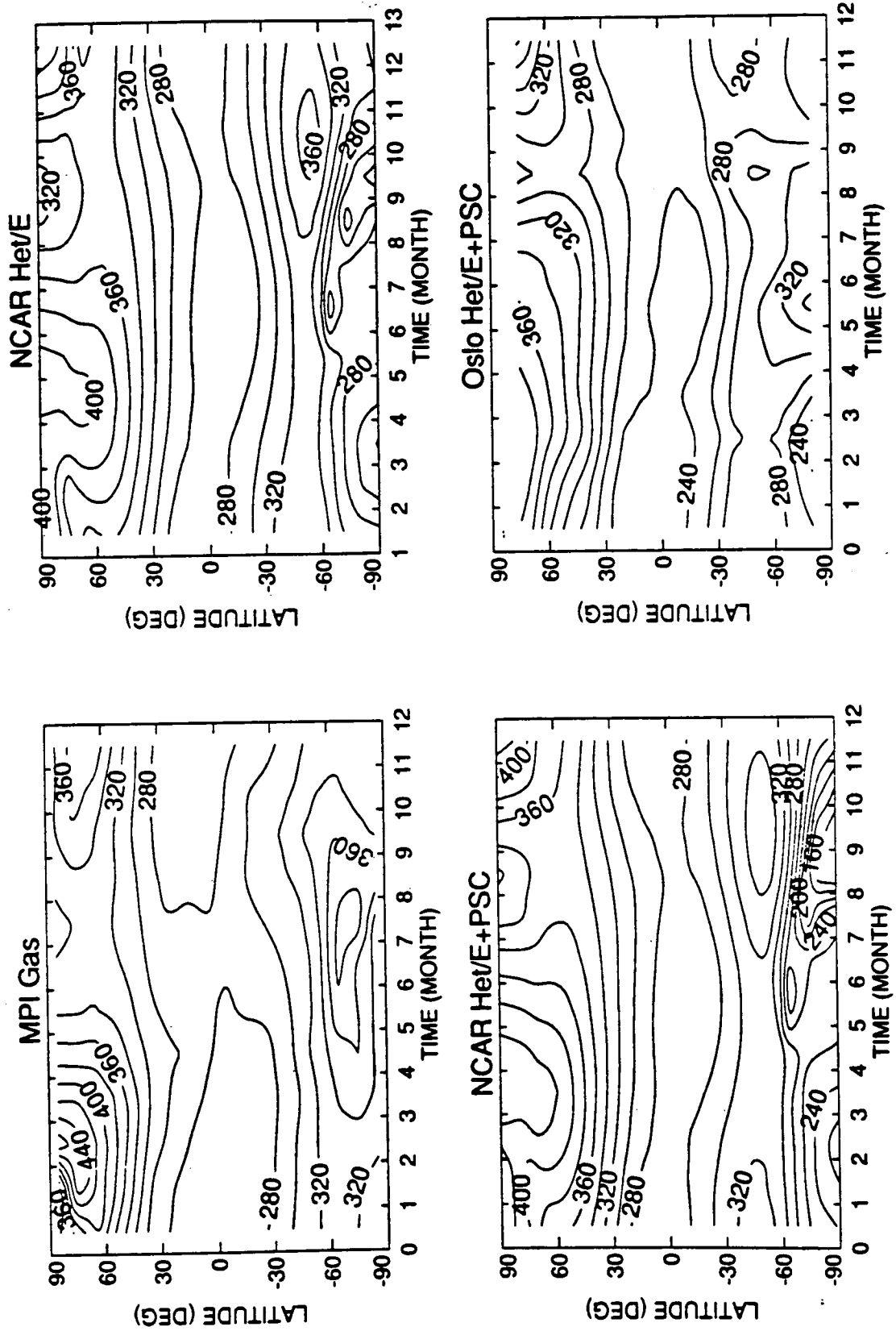


Figure 8-1c Column ozone abundances (Dobson Units) circa 1980 from observations (TOMS) and models.

FUTURE Cl-Br LOADING AND OZONE DEPLETION

Hemisphere maximum occurs in late winter to early spring at the pole; the Southern Hemisphere maximum occurs in early spring and is offset from the pole. The tropical minimum follows an annual cycle out of phase with the sun, reaching a minimum in the northern tropics in December. Only models with PSC simulations or specified polar ozone loss show the pattern typical of the Antarctic ozone hole in the Southern Hemisphere.

The contrast in column O_3 among models is large, but within a model the differences between the GAS and HET chemical formulations are usually small (not shown). For the 1980 simulations, most GAS models are no more than 4 percent different than corresponding HET models everywhere except in the Antarctic spring. In general, the differences among models and chemical formulations for column ozone cannot be used to discriminate among the models by comparison with observations for 1979 and 1980 alone. A better chance to test these simulations may be with the decadal trends discussed in the next section. More detailed analyses of the observations, their uncertainties, and year-to-year variations, along with objective measures of model accuracy, are planned as a workshop in 1992.

The distribution of ozone concentrations with altitude (*i.e.*, profiles) as a function of latitude and month can provide an additional test of the stratospheric models. In Figure 8-2, we show a mean measured profile for the month of March by combining observations from the Solar Backscatter Ultraviolet Spectrometer (SBUV) and the Stratospheric Aerosol Gas Experiment (SAGE II) from the early 1980s. This figure also shows results from the various models and chemical formulations as in Figure 8-1. A first-order comparison of the models with the observations shows very good agreement. For example, the largest ozone mixing ratios, about 10 to 11 ppm, are observed at about 33 km over the equator. The models' predictions are slightly less, 8 to 11 ppm, and the maximum occurs 1–2 km lower. In the upper stratosphere away from the poles, there has been a long-standing problem with the prediction of too low ozone mixing ratios, but here we see only a small, possibly systematic underprediction: at 40 km the observations show 8 ppmv and the models vary from 6 to 8 ppm; and at 50 km the observations are about 3 ppmv with the models varying from 2 to 3 ppm. For observations and many models, the 6-

ppmv contour closes off the volume from about 60°S to 60°N over the altitude range from about 28 to 40 km. Differences between GAS and HET in the same model would not be readily discernible in these contours. Large differences between models occur in the lower stratosphere (and are readily seen in Figure 8-2) due to variations among models in the rate of mixing and in the location of the tropopause. A more critical comparison and verification of these models awaits the 1992 workshop on models and measurements.

8.3.3 Modeled Ozone Depletion: 1980 to 1990

The observed reductions in column ozone from the Dobson network and the TOMS satellite (see Chapter 2) have focused attention on the model predictions of ozone change over the past two decades (see WMO, 1990a). The recent TOMS picture of the statistically analyzed decadal trend in column ozone (NOT the difference between years 1990 and 1980) is shown in Figure 8-3 along with model simulations of this change. The TOMS analysis has removed the effects of the solar cycle and thus should be directly comparable to the model simulations. The observations show largest decreases at middle and high latitudes during early spring with little or no significant trend in the tropics. The largest ozone depletions (30 percent) are associated with the Antarctic ozone hole, but substantial declines, more than 8 percent, occur in the Northern Hemisphere as far south as 40°N latitude.

Model calculations of the period 1980–1990 with gas phase chemistry only universally show very small decreases, if any, in column ozone: less than 1 percent change over the tropics and much of the mid-latitudes; peak losses of 2 to 3 percent only during late winter poleward of 60° latitude. When the HET chemical formulation is adopted, allowing for reactions on the sulfate layer, model calculations show substantially greater ozone loss for the period 1980–1990. Ozone losses at 45°N latitude in spring range from 3 to 5 percent in the Atmospheric and Environmental Research, Inc. (AER), Goddard Space Flight Center (GSFC), Lawrence Livermore National Laboratory (LLNL), National Center for Atmospheric

FUTURE Cl-Br LOADING AND OZONE DEPLETION

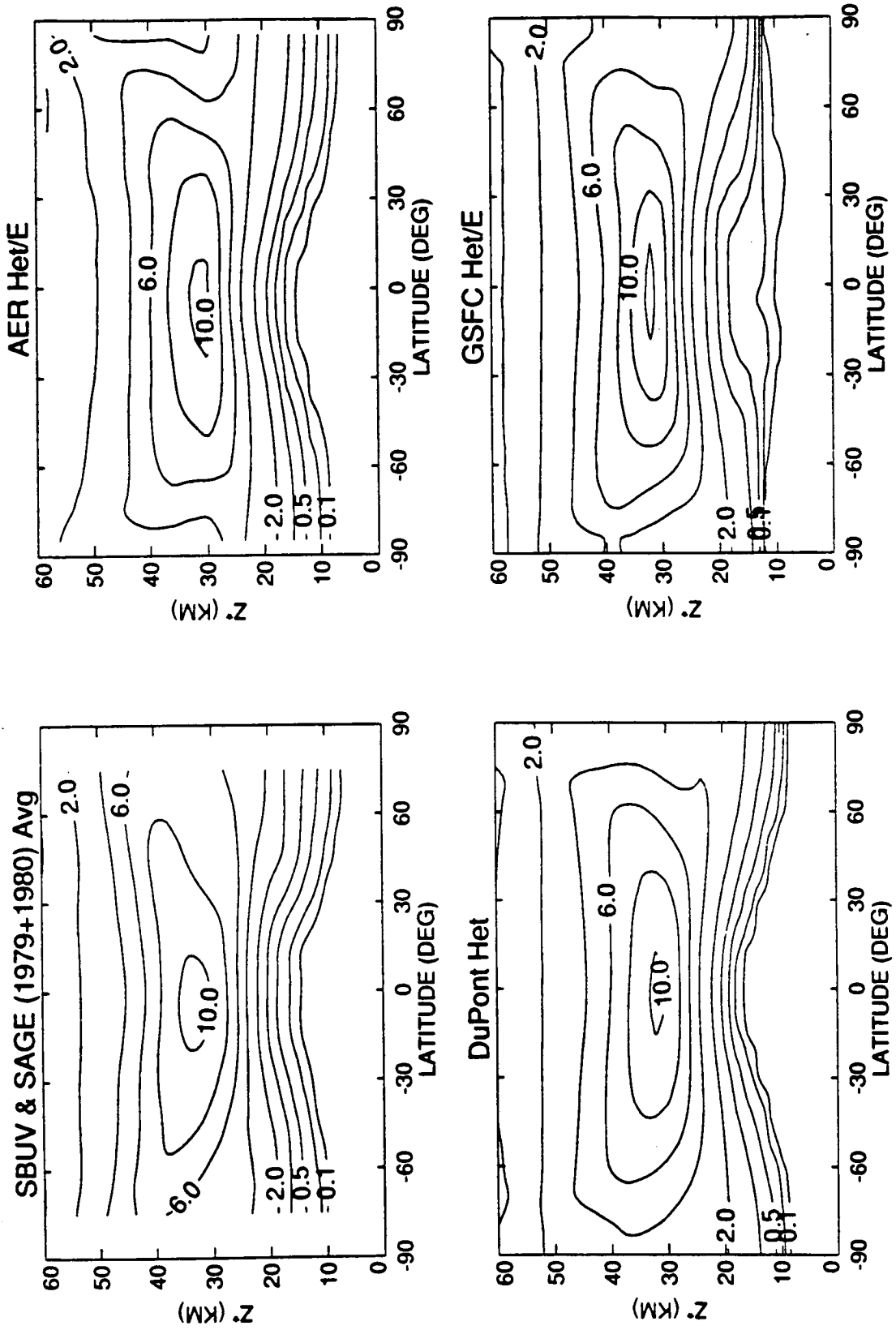


Figure 8-2a Ozone profiles (ppmv mixing ratio) circa 1980 from observations (SBUV) and models.

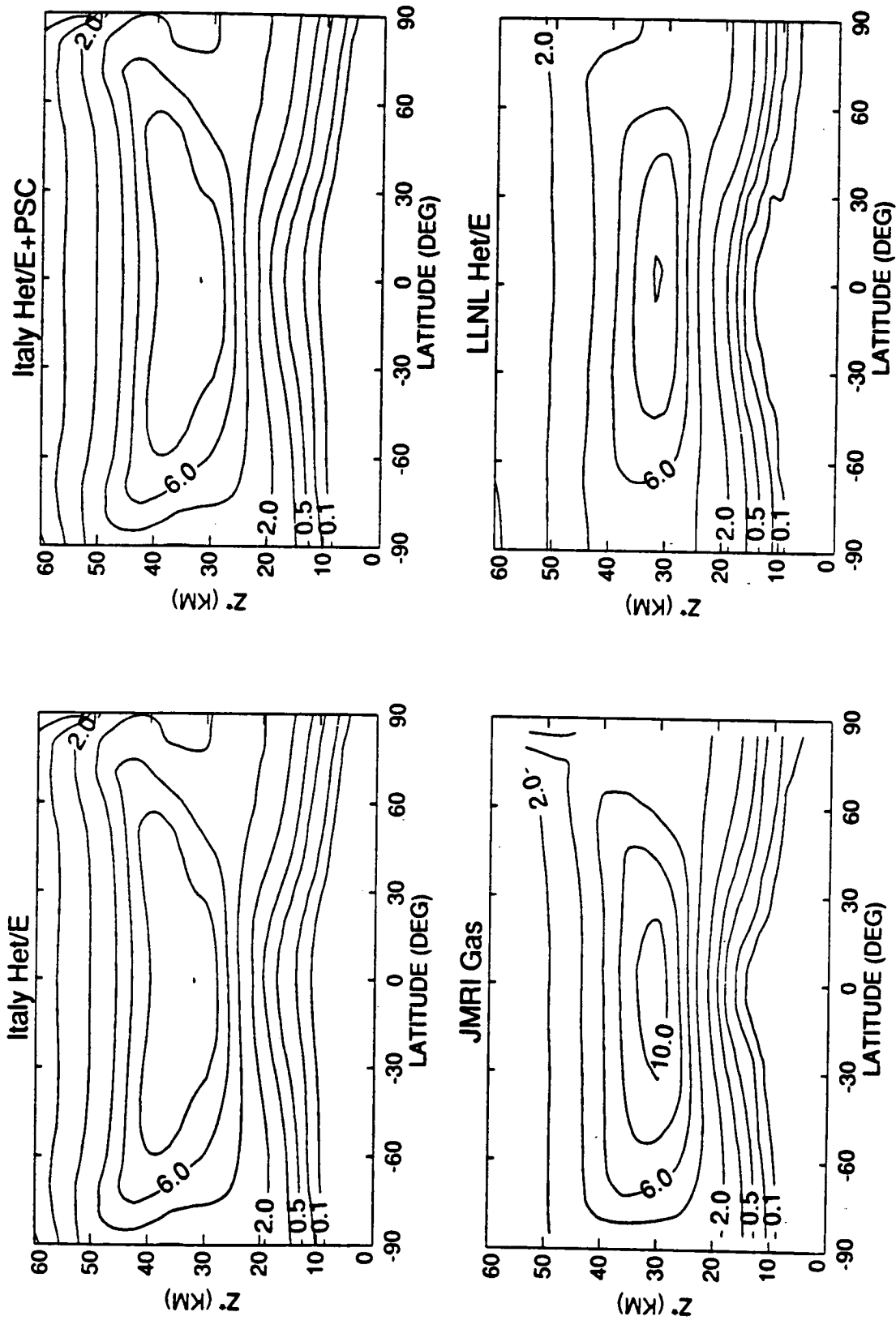


Figure 8-2b Ozone profiles (ppmv mixing ratio) circa 1980 from observations (SBUV) and models.

FUTURE Cl-Br LOADING AND OZONE DEPLETION

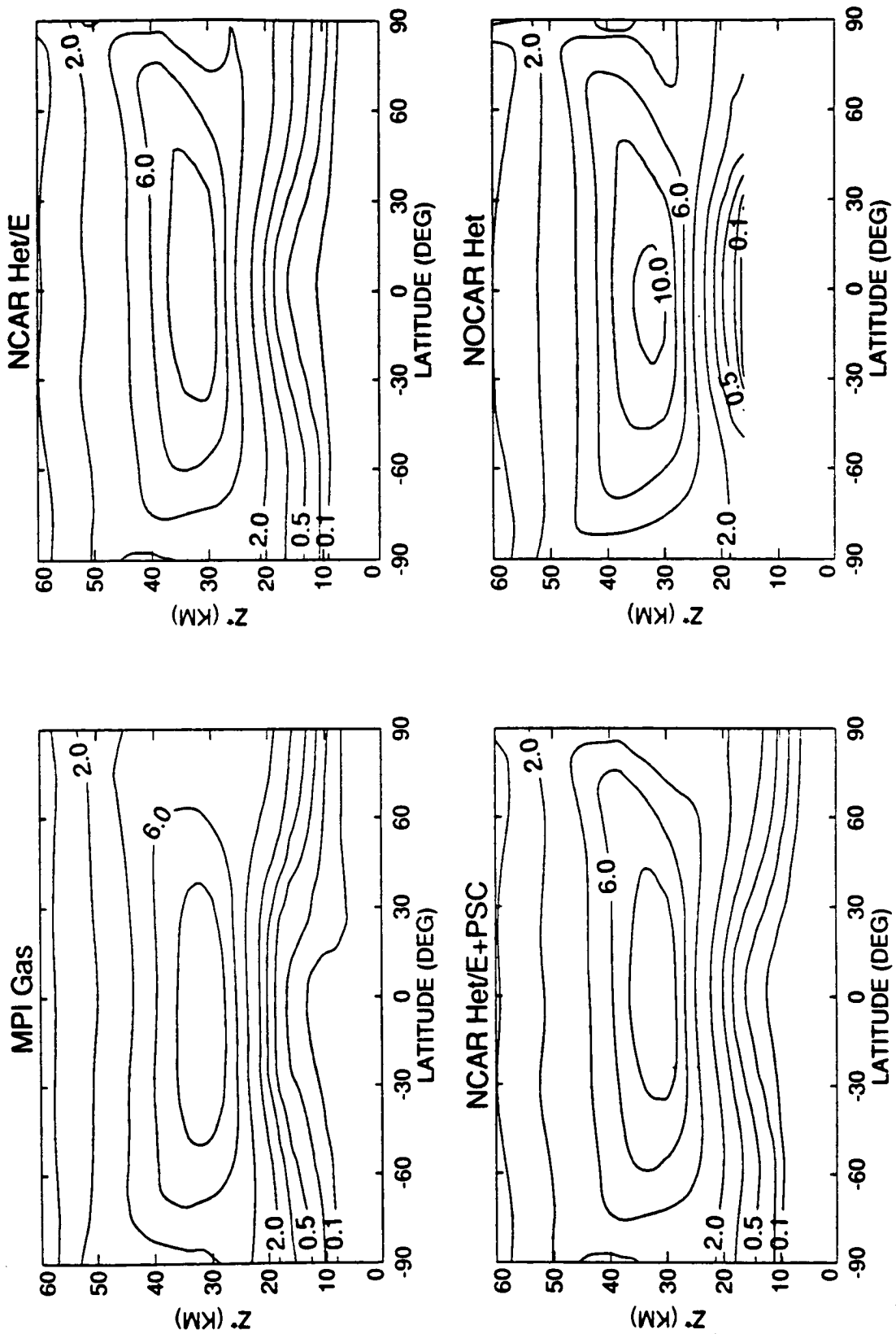


Figure 8-2c Ozone profiles (ppmv mixing ratio) circa 1980 from observations (SBUV) and models.

FUTURE Cl-Br LOADING AND OZONE DEPLETION

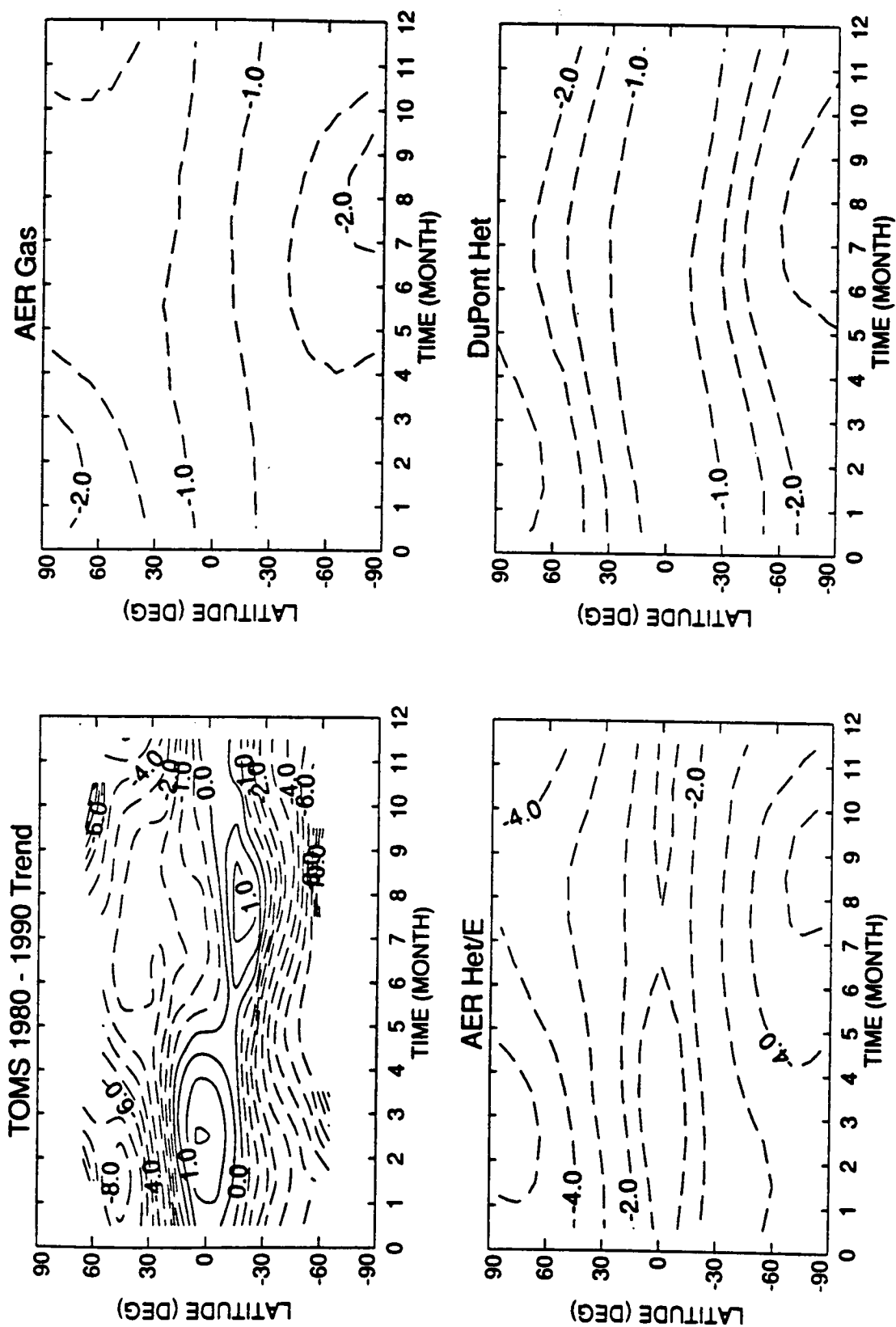


Figure 8-3a Change in column ozone abundances (percent) from 1980 to 1990 based on observations (TOMS) and models.

FUTURE Cl-Br LOADING AND OZONE DEPLETION

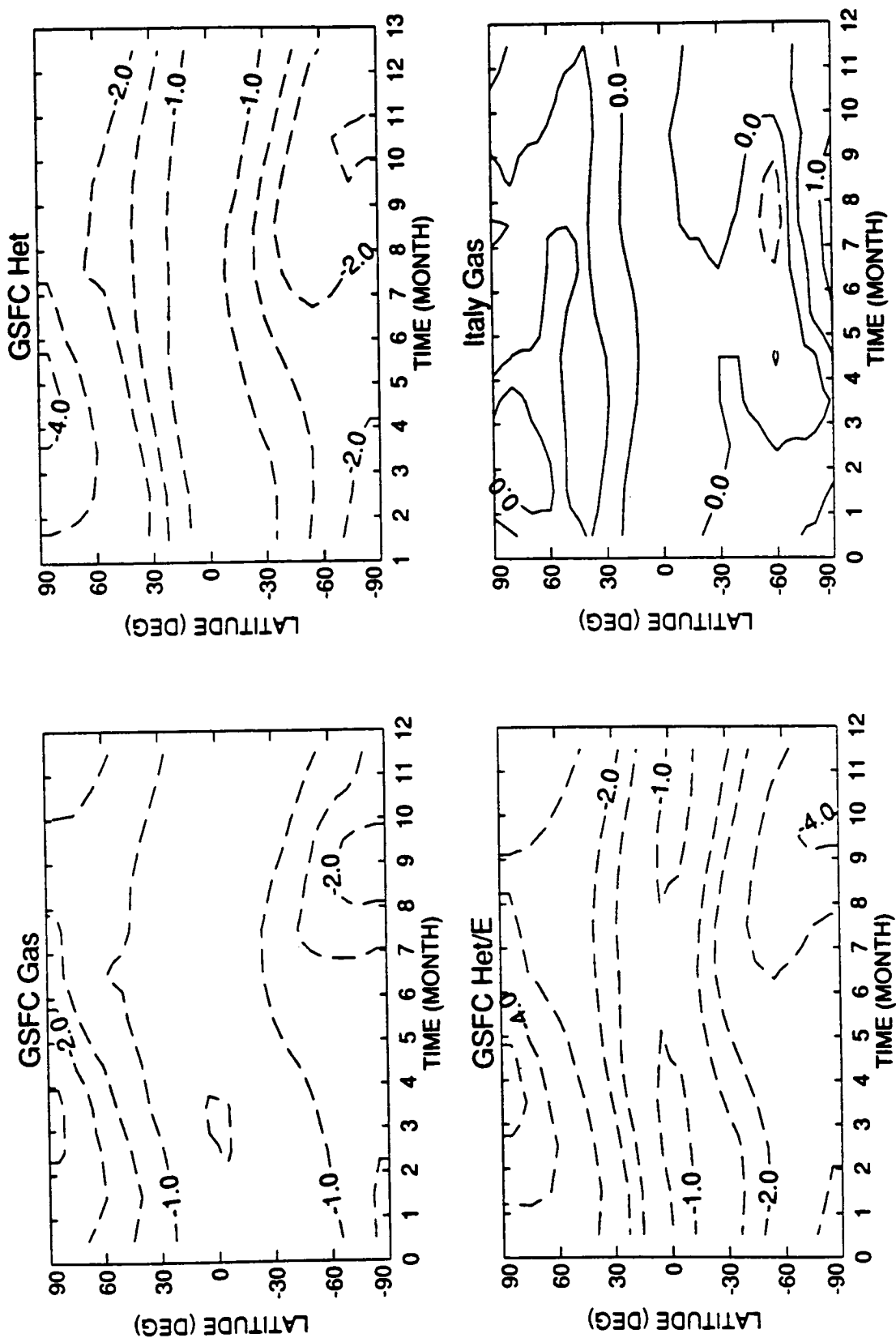


Figure 8-3b Change in column ozone abundances (percent) from 1980 to 1990 based on observations (TOMS) and models.

FUTURE Cl-Br LOADING AND OZONE DEPLETION

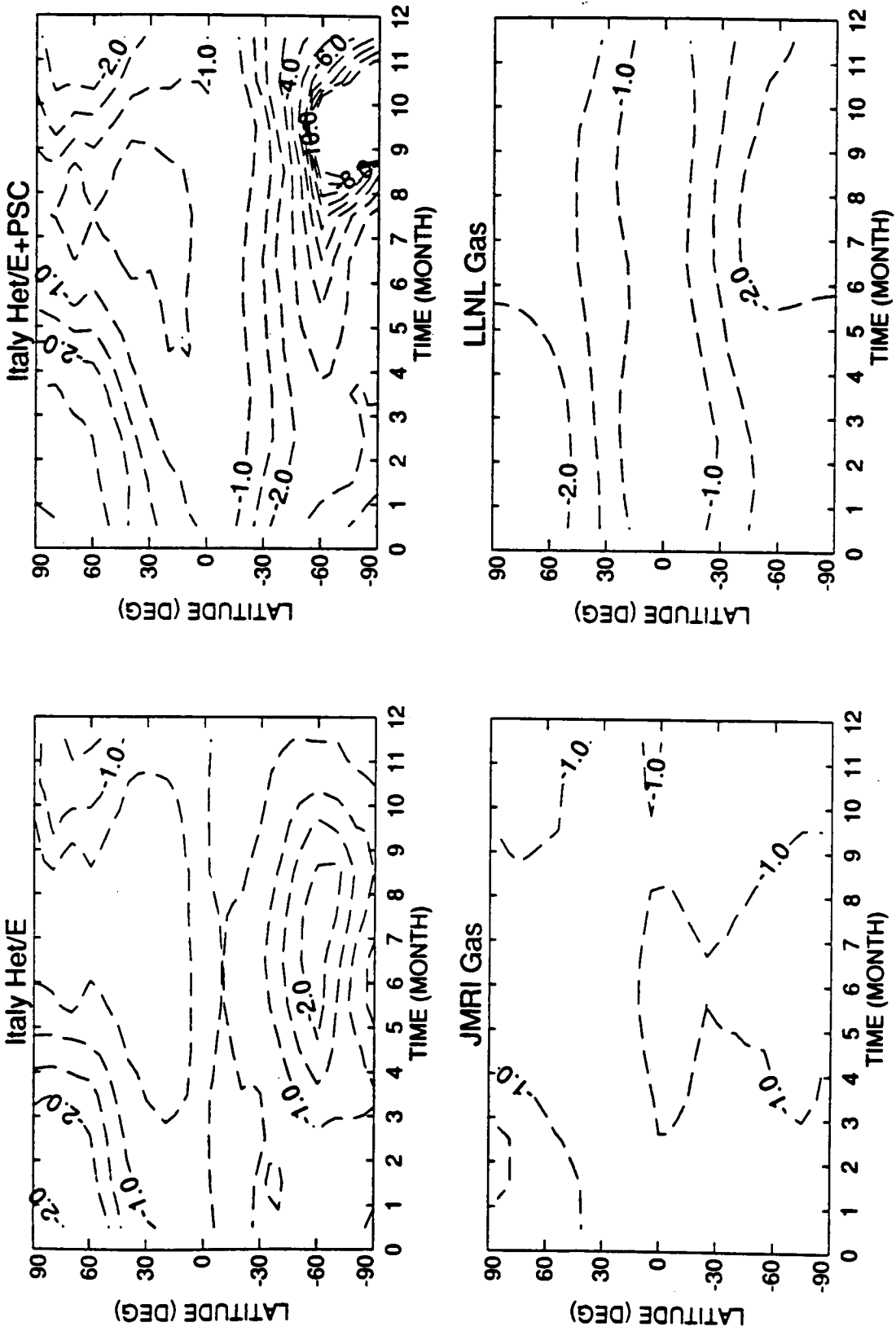


Figure 8-3c Change in column ozone abundances (percent) from 1980 to 1990 based on observations (TOMS) and models.

FUTURE Cl-Br LOADING AND OZONE DEPLETION

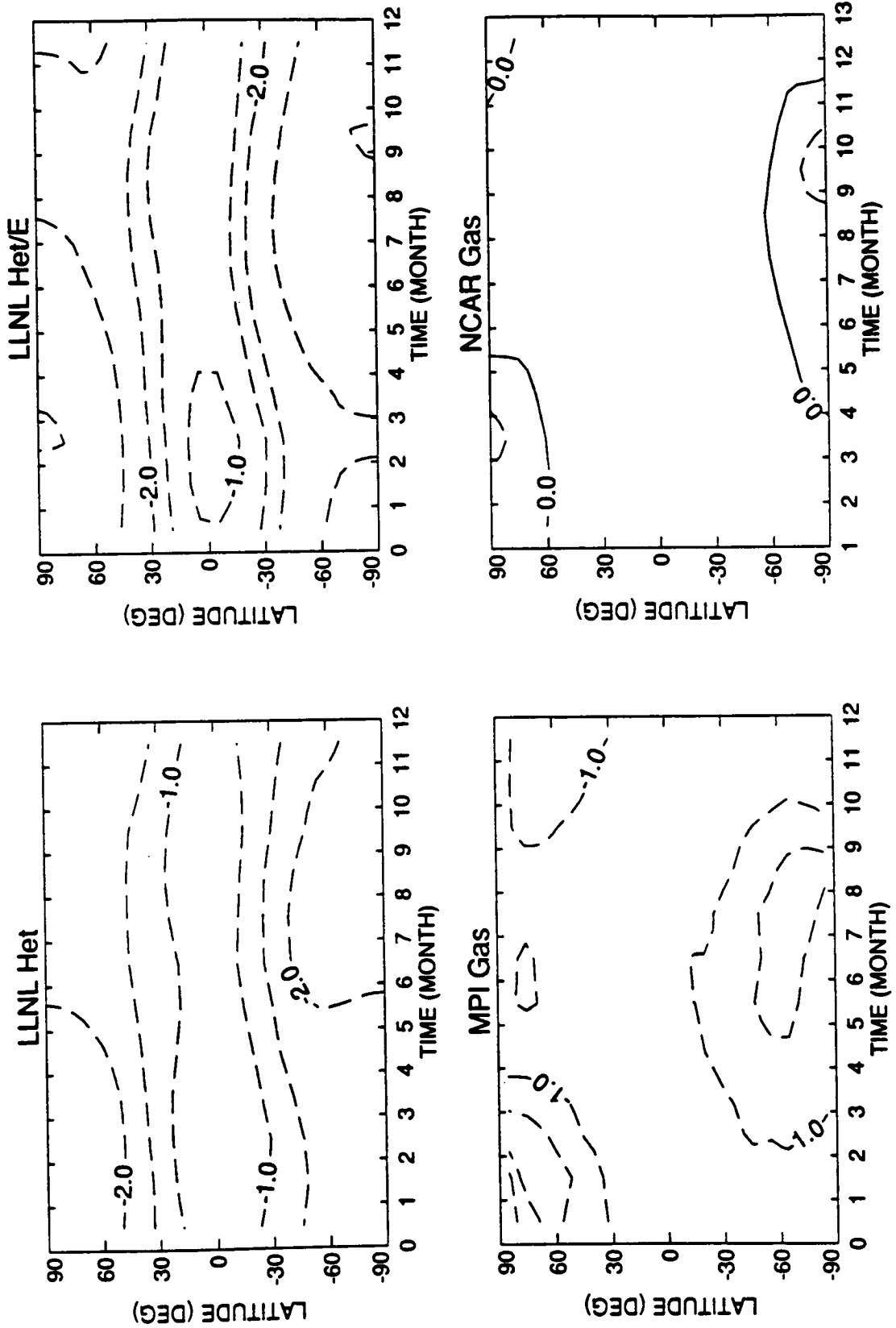


Figure 8-3d Change in column ozone abundances (percent) from 1980 to 1990 based on observations (TOMS) and models.

FUTURE Cl-Br LOADING AND OZONE DEPLETION

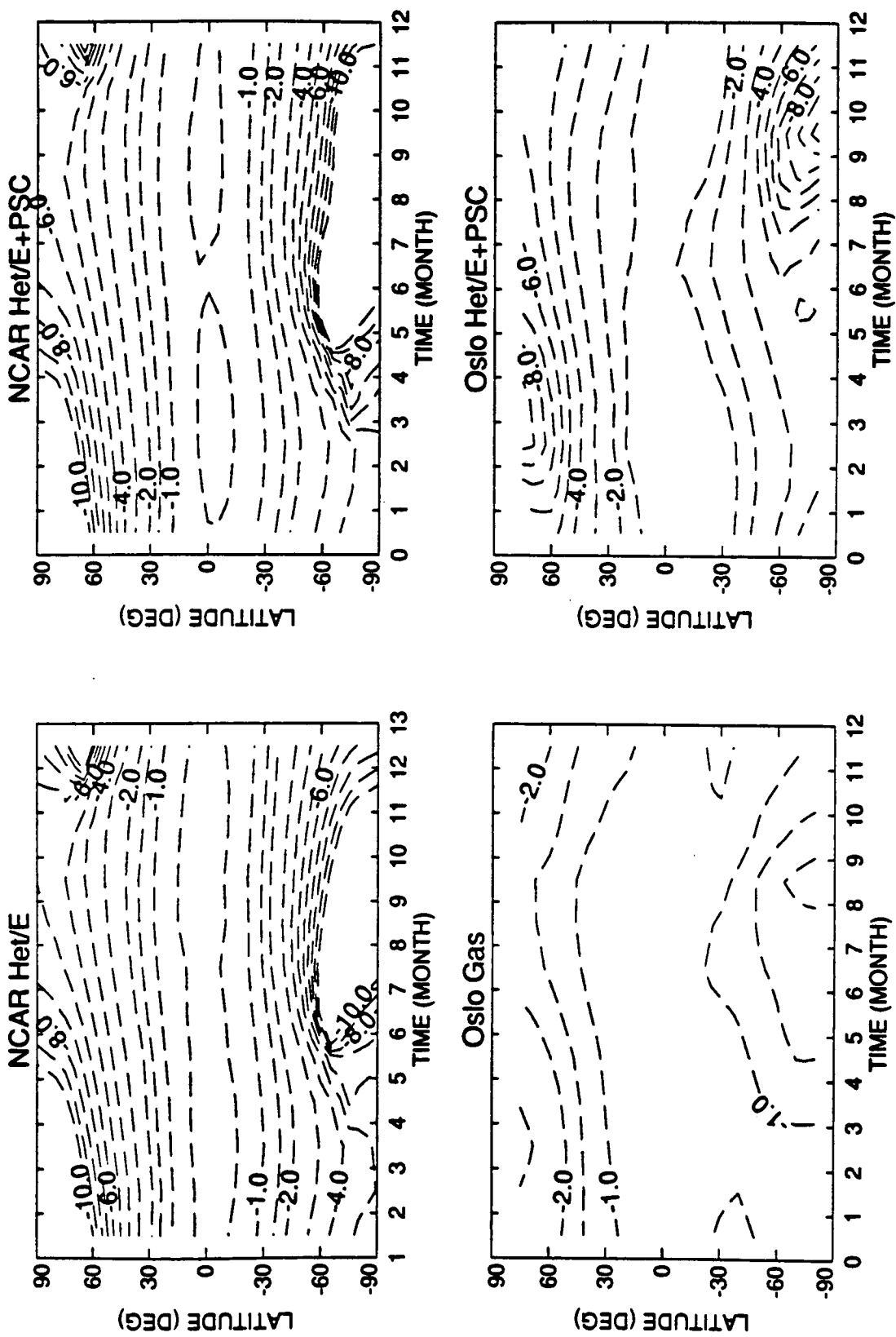


Figure 8-3e Change in column ozone abundances (percent) from 1980 to 1990 based on observations (TOMS) and models.

FUTURE Cl-Br LOADING AND OZONE DEPLETION

Research (NCAR), and Oslo models, and they are smaller but of similar pattern in the ITALY model. All HET models predict greater percentage losses at the poles. Most of the HET formulations predict 1 to 2 percent ozone depletion in the tropics over the decade; these values are larger than derived from TOMS, but fall within the quoted uncertainties (see Chapter 2).

The difference in predicted ozone depletion between the upper and lower limits of sulfate aerosol area is of some interest in view of the large variations, factor of 40 or more, in the sulfate layer over the past decade in response to volcanic eruptions. For example, most models (*e.g.*, AER, GSFC, and LLNL) show that the factor of 4 increase in surface area results in about a 1/2 percent larger ozone depletion over most latitudes and seasons. Therefore, model predictions for a 40 percent shift in the baseline value of sulfate layer area over this period would show negligible effects.

In general, the GAS models predict integrated column depletions and vertical profiles of ozone loss from 1980 to 1990 that are much less than those observed at middle latitudes over all seasons in both hemispheres. The HET models simulate most of the observed column ozone loss from 1980 to 1990 for the northern middle latitudes in summer, but only about half of that in winter (see Table 8-A). At high southern latitudes, however, the HET models fail to predict the massive losses associated with the Antarctic ozone hole (PSC chemistry), but still can explain part of the loss at southern mid-latitudes.

Three PSC models incorporate a parametric formulation of the chemistry involving PSCs; however, these PSC simulations in two-dimensional models remain incomplete. While PSC models are still under development, current versions predict greater ozone loss at northern middle latitudes in winter and early spring than do the GAS or HET models. It is possible that the combination of HET and PSC chemistries is synergistic and not linear, and thus, we cannot treat results from the two types of models as additive.

Modeled changes (percent) in the ozone profiles for the decade 1980–1990 are shown in Figures 8-4a-d. The month of March was selected for this comparison because it corresponds generally to the time of maximum ozone loss in the Northern Hemisphere. In this case, the observations are not yet sufficient to

report with any degree of certainty the decadal changes in local ozone concentrations resolved latitudinally and monthly. For reference, see Chapter 2 where the observed trends in ozone profiles are reported only at individual stations (Figure 2–12 shows Payerne data) or as averages over latitudes and/or seasons (Figures 2–13 and 2–14 show SAGE data annually averaged).

Ozone depletion from March 1980 to March 1990 is calculated to have a distinct signature or fingerprint. Greatest losses, 12 to 16 percent, occur at high latitudes of both hemispheres (60° to 90° latitude) at the stratopause (40 to 50 km). One exception to this is the LLNL model with a similar pattern, but only 8 percent loss. (The smaller ozone loss in the LLNL model is in part consistent with the temperature feedback included in the model whereby ozone reductions lead to colder temperatures which in turn reduce the rates of ozone loss, especially in the upper stratosphere. When the LLNL model uses fixed temperatures [not shown], its results match those others shown here. However, the NCAR and NOCAR models shown here also include temperature feedback and still predict 12 to 16 percent losses. This discrepancy is unresolved.) Ozone depletion at the stratopause (about 45 km) is predicted to be much smaller in the tropics and at mid-latitudes, where it is slightly larger than, but still within the uncertainty of, the measured decrease (see Chapter 2).

Most models calculate a local ozone enhancement of 1 to 2 percent in the tropics somewhere between 18 and 25 km. This increase in ozone often extends down, into the troposphere, but has little effect on the column because of the small mixing ratios there (see Figure 8-2). At middle latitudes the difference between GAS and HET chemistries shows up clearly in lower stratosphere: in GAS the region 45°N to 90°N between 15 and 25 km has calculated depletions of at most 1 to 2 percent; whereas in HET the depletion in this region is expected to exceed 4 percent. (Not all models match this pattern.) Perhaps one of the most obvious signatures of heterogeneous chemistry (as proposed) is the bimodal pattern of ozone depletion at 50°N to 60°N with a minimum loss near 30 km that appears in all the HET calculations. Some GAS models also show ozone losses in the polar lower stratosphere, extending to mid-latitudes, due to rapid downward transport of ozone depletion from the upper stratosphere.

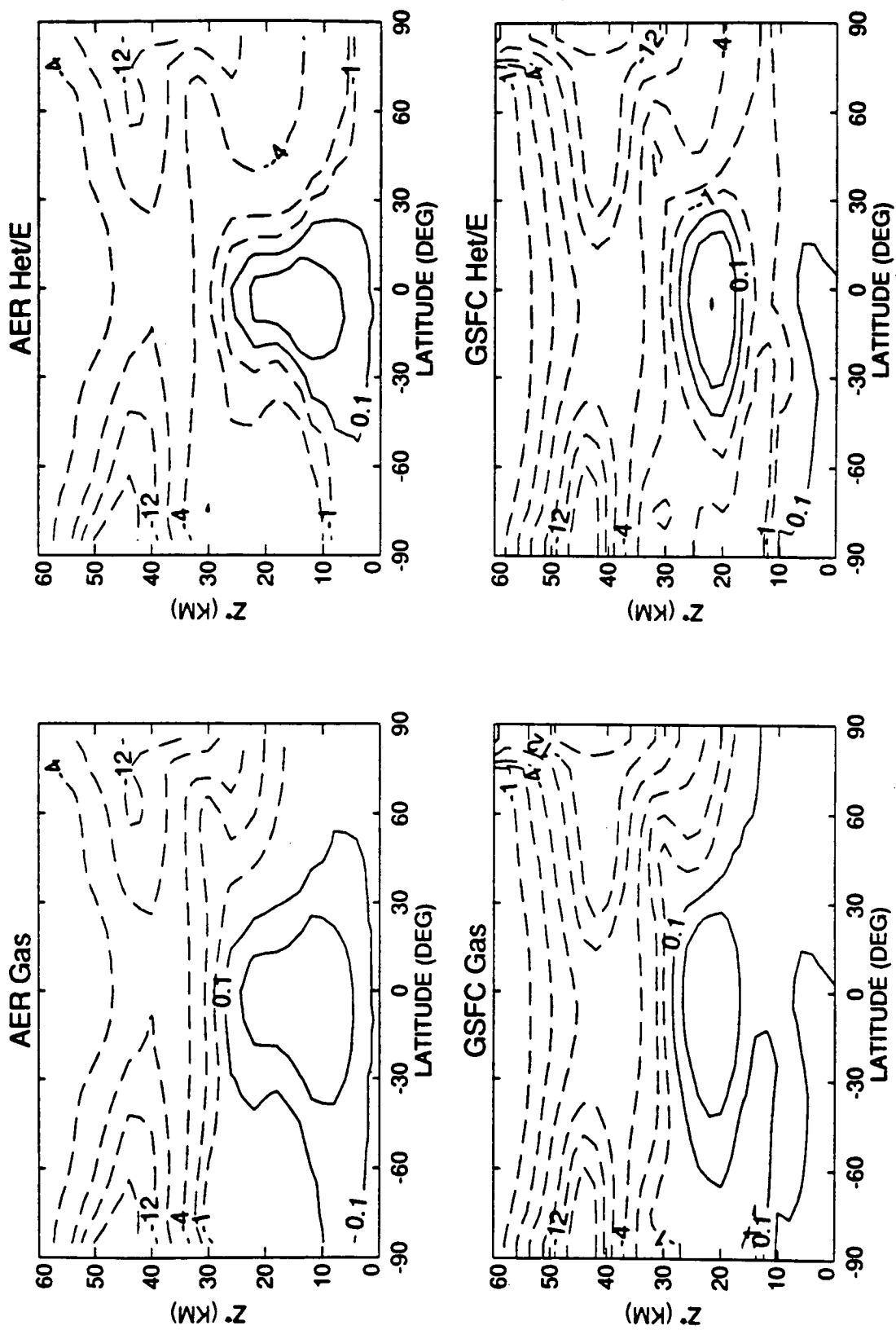


Figure 8-4a Change in ozone profiles (percent) from 1980 to 1990 from models.

FUTURE Cl-Br LOADING AND OZONE DEPLETION

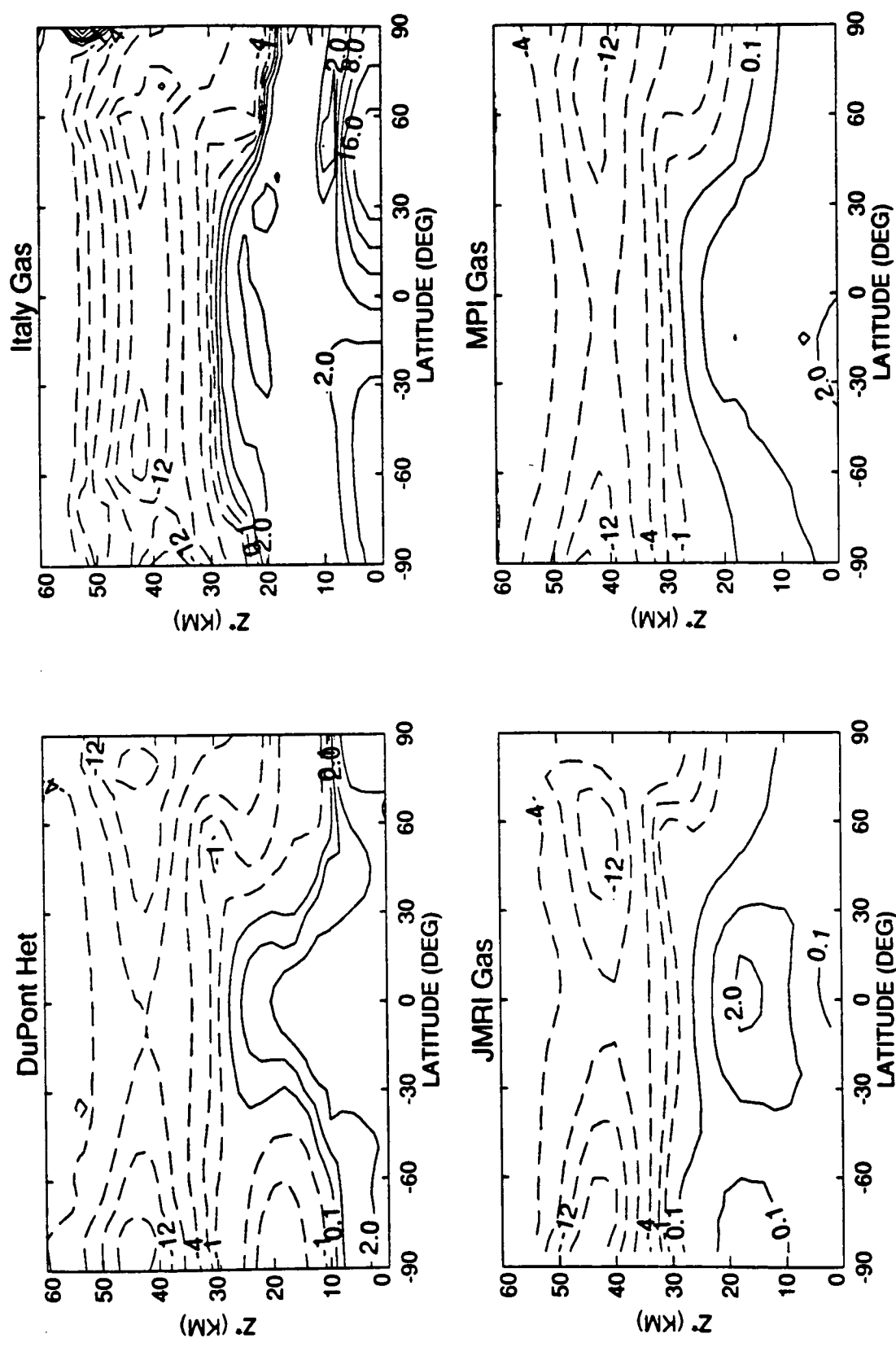


Figure 8-4b Change in ozone profiles (percent) from 1980 to 1990 from models.

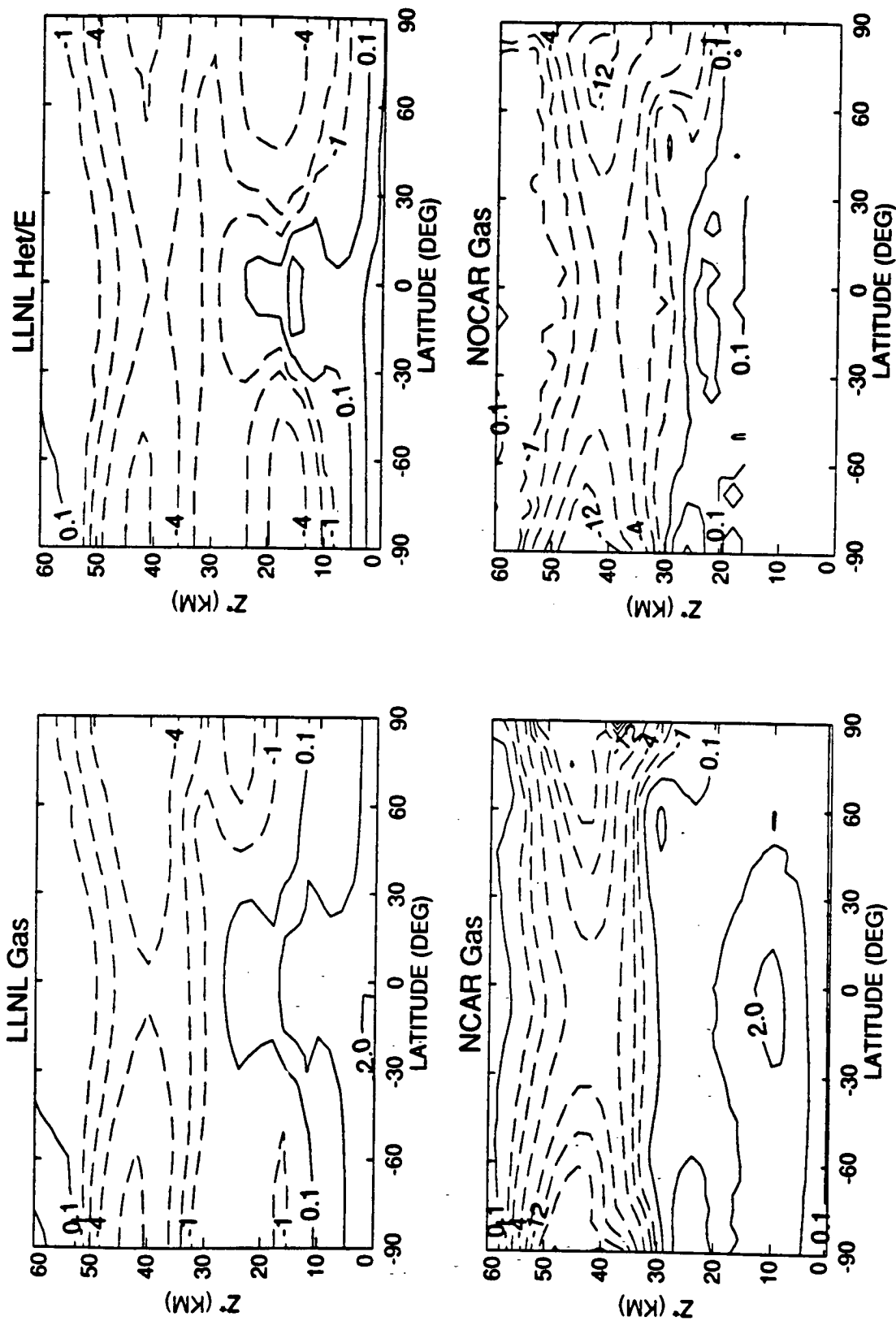


Figure 8-4c Change in ozone profiles (percent) from 1980 to 1990 from models.

FUTURE Cl-Br LOADING AND OZONE DEPLETION

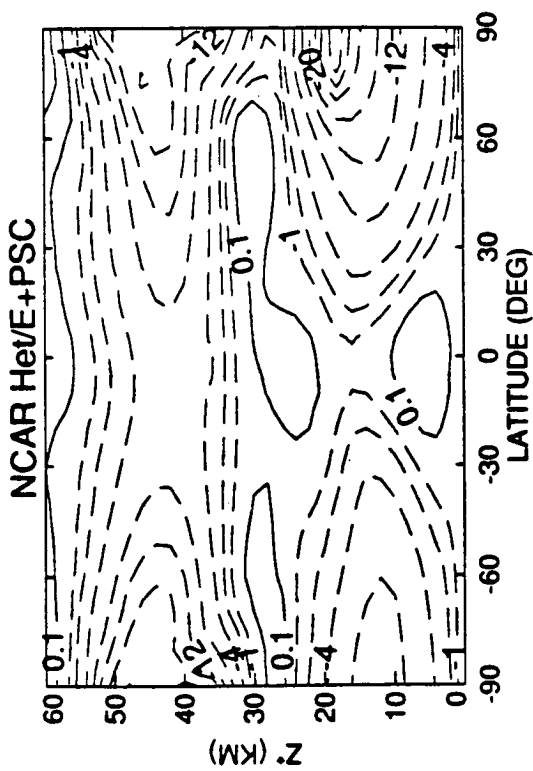
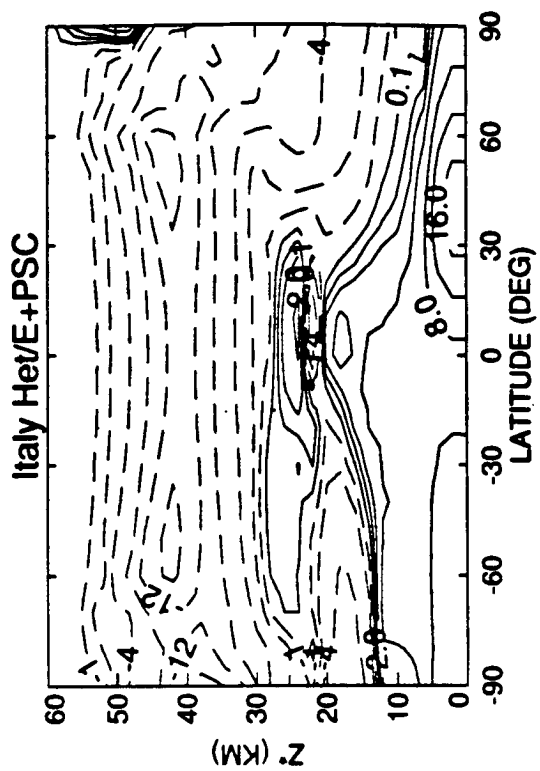


Figure 8-4d Change in ozone profiles (percent) from 1980 to 1990 from models.

FUTURE Cl-Br LOADING AND OZONE DEPLETION

Observed changes in ozone profiles over the past decade are not spatially and temporally resolved, as compared with the column changes, to provide a critical test of these simulations (see Chapter 2). Nevertheless, the observed change in ozone profile at mid-latitudes points to two modes of ozone loss, centered separately in the upper and lower stratosphere. The observed loss above 40 km altitude appears to be less than that predicted by models. This discrepancy is worrisome because the presumably well-known gas phase chemistry controls ozone in the upper stratosphere. The disagreement between model simulations and observations may easily fall within the uncertainties of the measurement of such trends (see discussion in Chapter 2). In the lower stratosphere, the agreement with the HET models in March may be fortuitous and cannot be used to verify the current chemical formulation because other mechanisms, particularly processing by PSCs in January and February, may lead to ozone depletion in March. An independent check might be to look for lower stratospheric ozone loss in September, before the occurrence of PSCs, but while the sulfate layer chemistry is active. Model simulations, however, predict a smaller effect and less distinctive signature in September.

8.4 PREDICTING THE FUTURE ATMOSPHERE: 1990-2050

The prediction of the future state of the stratosphere is first examined as semicontinuous time lines of scalar quantities such as chlorine and bromine loading. Then we study the magnitudes and patterns of calculated ozone change as we pass through the maximum in chlorine loading (circa 2000) described in Scenarios A-C.

8.4.1 Time Lines of Change

The chlorine and bromine loading of the atmosphere as defined in the scenarios of Tables 8-3 and 8-6a are plotted in Figures 8-5a and b. These figures include the extension of the scenarios to 2100. Scenario M is an optimistic, unrealizable baseline, assuming that the revised phaseout of the protocol (Table 8-4) meets with absolute global compliance (including all currently unregulated industrial halocarbons). A parallel case shows predictions for

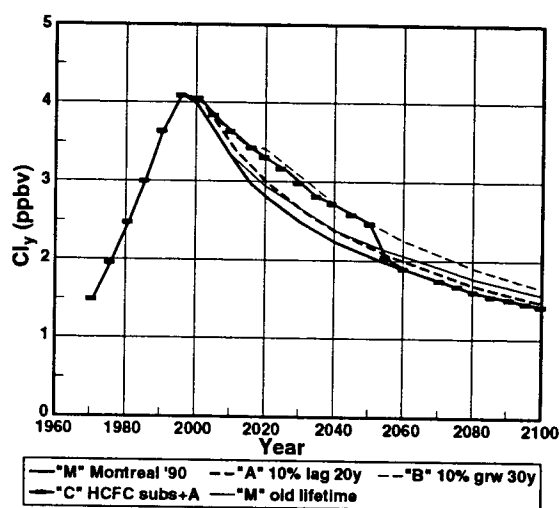


Figure 8-5a Chlorine loading for the basic scenarios (see Table 8-5).

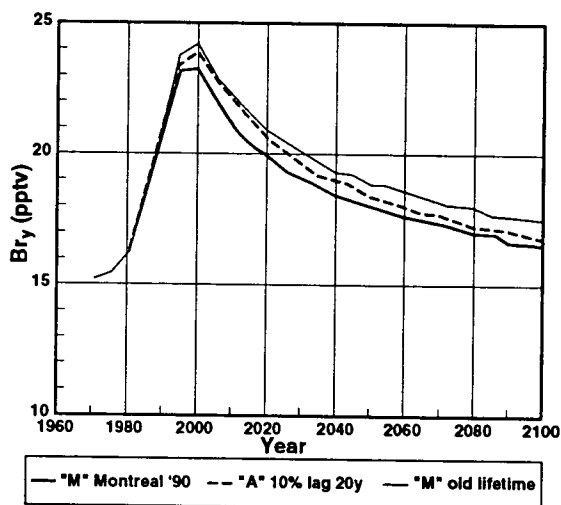


Figure 8-5b Bromine loading for the basic scenarios (see Table 8-5).

the identical scenario, but using the longer lifetimes (e.g., 60 years for CFCl_3) adopted in the previous assessments (WMO, 1990b; Prather and Watson, 1990). For chlorine, the effect of CFC lifetimes is not discernible until 2010, but the difference grows steadily. This spread is not an estimate of the uncertainty in predictions of future chlorine loading (see Prather and Watson, 1990), since the uncertainty in CFC lifetimes is greater than the 10 percent

FUTURE Cl-Br LOADING AND OZONE DEPLETION

difference in these two cases (see Table 8-1). Furthermore, we must fold in the uncertainties in future CFC emissions. In the case of bromine, the uncertainty in halon lifetimes is manifest by the year 2000.

Scenario A, the optimistic phaseout with 10 percent of the market given a 20-year delay, parallels Scenario M with 0.1 to 0.2 ppbv greater chlorine levels throughout most of the 21st century. Scenarios B and C are basically similar out to the year 2050, having the same chlorine loading (up to 0.4 ppbv greater than in A), but from quite a different suite of halocarbons. The chlorine in Scenario B is due to CFCs and is committed for the better part of the century even though emissions cease in the year 2020. By 2050, the difference between Scenarios C and A is due mostly to short-lived HCFCs, and the recovery can be swift, less than 5 years, if emissions are halted. The growth of HCFC substitute H_y in Scenario C continues, perhaps to excess, reaching almost 7 megatons/year in the year 2100; all other scenarios have eliminated halocarbon emissions by the year 2020.

The propagation of chlorine into the stratosphere is shown with the AER and SPB models in Figure 8-6. In steady state, the tropospheric chlorine loading includes all halocarbons and peaks at 4.1 ppbv in

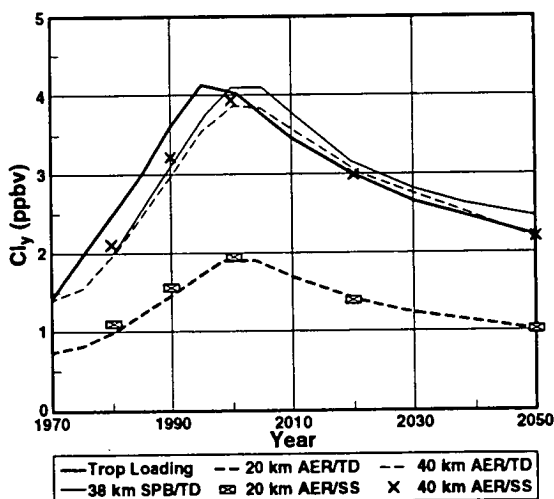


Figure 8-6 Chlorine levels at mid-latitudes (40–50N) in March. The tropospheric chlorine loading is compared with the lag in response predicted with the time-dependent AER results. Steady-state results from AER and SPB model also shown.

1995. The stratospheric Cl_y mixing ratio is always less than the tropospheric chlorine loading because not all the halocarbons are destroyed. At 40-km altitude, the Cl_y levels peak at 3.9 ppbv about 5 years after the chlorine loading; at 20-km altitude, they may peak a little earlier, but are much lower, about 2 ppbv. Also shown are the chlorine levels calculated with the same model using the steady-state atmospheres prescribed in Table 8-6b. Both approaches lead to similar histories of stratospheric Cl_y .

A comparison of the AER and GSFC model predictions of Cl_y and Br_y ($Br + BrO + HBr + BrONO_2 + HOBr + BrCl$) in northern mid-latitudes (40°N–50°N) is shown in Figure 8-7 for Scenario A. Both models predict similar magnitudes and time lags

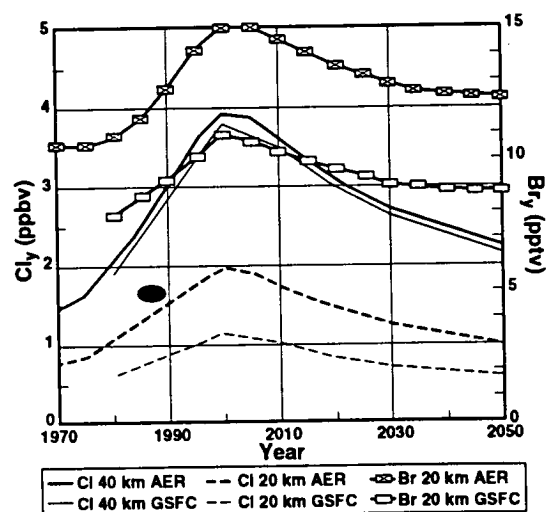


Figure 8-7 Chlorine and bromine levels at 40–50N in March from the AER (thick lines) and GSFC (thin lines) models. Cl_y estimates (oval) at 20 km from Schmidt *et al* (1991).

in Cl_y at 40-km altitude, but the lower stratospheres of these two models are dramatically different as noted in the general intercomparison of ozone profiles. The GSFC model has 30 percent less Br_y and almost 50 percent less Cl_y at 20-km altitude; O_3 levels from the two models (not shown) are, however, similar. At 20 km, it appears that the AER model has more photochemically processed air, while the GSFC model retains more of the chlorine in the form of halocarbons. Such differences should have an impact on the predicted ozone changes.

FUTURE Cl-Br LOADING AND OZONE DEPLETION

The impact of the HET chemical formulation is shown in Figures 8-8 for Scenario A with both the AER and GSFC time-dependent calculations. The maximum ozone depletion at 40-km altitude near 45°N latitude differs from model to model but peaks at about 20 percent in the year 2000 and is identical for both GAS and HET chemistries since sulfate layer

chemistry takes place only at lower altitudes. At 20-km altitude, the picture is quite different. For GAS, the initial trends from the two models have different signs, but the long-term trends from years 2010 to 2050 is similar. This latter decline (while chlorine is recovering) is attributed to increasing NO_y . For HET, the initial decline in ozone corresponds to the rapid

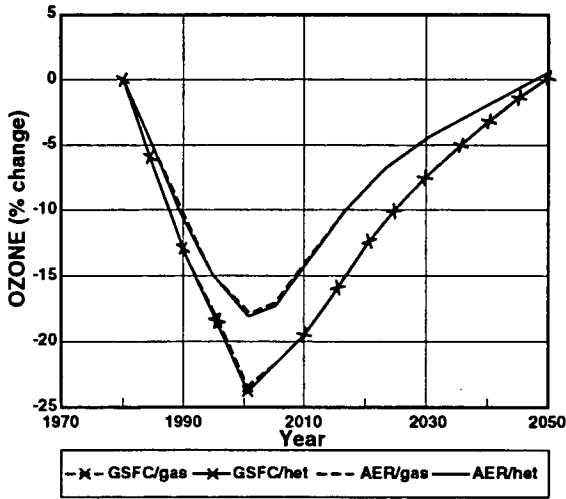


Figure 8-8a Ozone changes (percent) at 40 km, 45N in March from AER (line) and GSFC (X-line) for scenario A using GAS (dashed line) and HET (solid line) models.

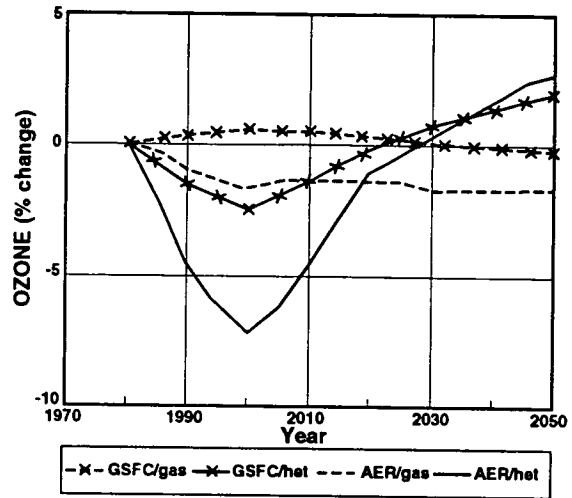


Figure 8-8b Ozone changes (percent) at 20 km, 45N in March from AER (line) and GSFC (X-line) for scenario A using GAS (dashed line) and HET (solid line) models.

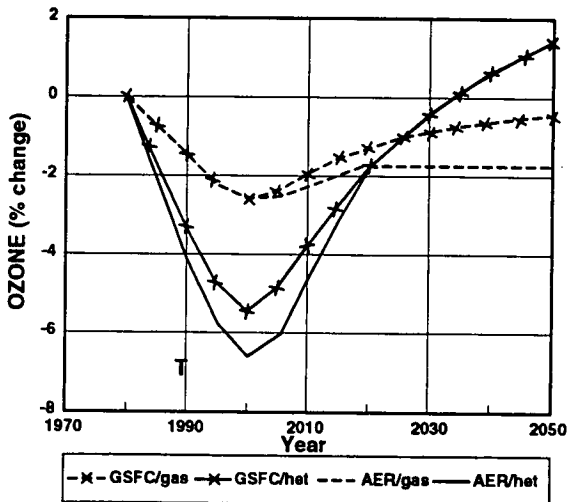


Figure 8-8c Ozone column change (percent) at 45N in March from AER (line) and GSFC (X-line) for GAS (dashed) and HET (solid) models. TOMS trend shown as a 'T'.

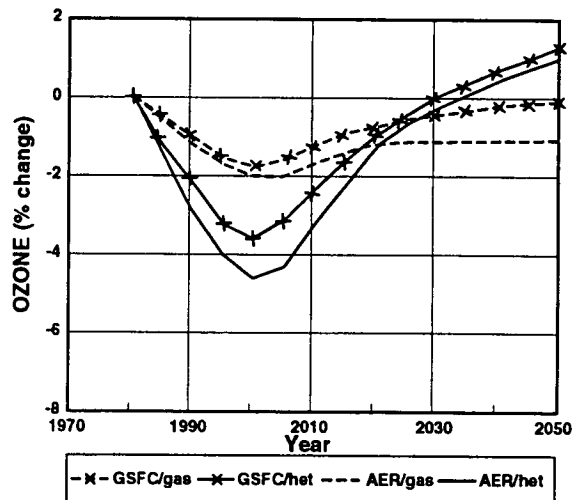


Figure 8-8d Ozone column change (percent) annually averaged Northern Hemisphere, from AER (line) and GSFC (X-line) for GAS (dashed) and HET (solid) models.

FUTURE Cl-Br LOADING AND OZONE DEPLETION

rise in Cl_y at 20 km; however, the recovery of O_3 proceeds faster than that of Cl_y because of CH_4 and NO_y increases. The ozone column abundances near 45°N reflect both the 20-km and 40-km patterns; for GAS both models predict a maximum loss of -2.5 percent in the year 2000 followed by a slow recovery; for HET the maximum column loss is about -6 percent and the recovery is much more rapid. In the GAS formulation, the column ozone never recovers because the NO_y increases lead to ozone depletion by 2050. In the HET formulation the recovery of the ozone column is rapid, becoming positive after the year 2030. The average ozone column over the Northern Hemisphere shows a similar history, but with a smaller amplitude.

The recovery of O_3 in the 21st century is clearly different in the GAS and HET chemistries. The explanation comes from an understanding of the relative importance of the different catalytic cycles that destroy ozone in the lower extratropical stratosphere (45°N - 90°N , 14 to 23-km). Two models, designated as AER/GSFC, have analyzed the components of ozone loss for the year 2000. For GAS, the NO_y -related cycles account for 57/50 percent of the total, Cl_y -cycles for 6/4 percent, Br_y -cycles (including $\text{BrO} + \text{ClO}$) for 4/4 percent, HO_x for 25/30 percent, and O_x (Chapman cycle) for 8/12 percent. The corresponding values for HET are 19/16 percent for NO_y , 18/8 percent for Cl_y , 10/22 percent for Br_y , 45/46 percent for HO_x , and 8/8 percent for O_x . With the traditional GAS chemistry, the NO_y cycles are the most important ozone loss processes in the lower stratosphere, and thus the increase prescribed for N_2O leads to small ozone column reductions in the year 2050, even after Cl_y has recovered. With HET chemistry the impact of the Cl_y changes is amplified, and the recovery to positive values for the ozone column reflects the fact that ozone columns in 1980 (our reference year) are probably depressed by 2 to 4 percent relative to the pre-ozone hole conditions (early 1970s). Also, for HET the changes in N_2O have a much smaller impact on ozone, but CH_4 (through the HO_x chemistry) becomes more important.

Overall, with HET chemistry the role of NO_y in the stratosphere is reduced (Rodriguez *et al.*, 1991; Pitari *et al.*, 1991) because the fraction of NO_y in the active forms, NO and NO_2 , is much smaller. The reaction of N_2O_5 on sulfate particles is the critical

reaction in HET for most of the models. A sensitivity study with the AER model shows that the much slower ClONO_2 -sulfate reaction acting alone, or added to the N_2O_5 -sulfate reaction, has only a minor impact on ozone: a few tenths of percent in local concentrations and about 0.1 percent in the column. This result is not necessarily universal, since the NCAR model, which includes a parametric model of PSC chemistry, reports that the ClONO_2 reaction is important.

The importance of bromine in these calculations is small, almost trivial, for the GAS models, but is enhanced for the HET models. The catalytic loss of O_3 by the $\text{BrO} + \text{ClO}$ reaction rises as ClO concentrations rapidly increase following the reduction of NO_x by heterogeneous conversion to HNO_3 (Rodriguez *et al.*, 1991). A larger role for the Br_y -catalyzed loss of ozone is predicted for the lower stratosphere (14-23 km) when PSC processing is included, but cannot be quantified from the simulations here.

8.4.2 Patterns of Ozone Change

The largest changes in ozone are predicted to occur in the year 2000 when stratospheric chlorine levels peak in the scenarios adopted here. There is little difference between scenarios in the year 2000 and thus we focus on Scenario A. The predicted ozone column changes from the year 1980 to 2000 are mostly depletions in this case, and their patterns are shown in Figure 8-9. The GAS chemistry models predict modest losses ranging from 0 to 4 percent, whereas the HET models show ozone depletions several times larger. In all cases, the loss is maximal around the winter pole and minimal over the tropics.

The largest difference between Scenarios A, B, and C occurs in the year 2020. Results for the year 2020 are shown in Figure 8-10 for the HET GSFC model. It is important to examine the HET models here, since we know that the GAS models are insensitive to chlorine changes between the years 1980 and 1990 (similar to the spread in chlorine loading between Scenarios A, B, and C in 2020). Scenarios B and C lead to slightly larger column ozone depletions of x-y percent relative to Scenario A, with differences between Scenarios B and C being slight.

FUTURE CI-Br LOADING AND OZONE DEPLETION

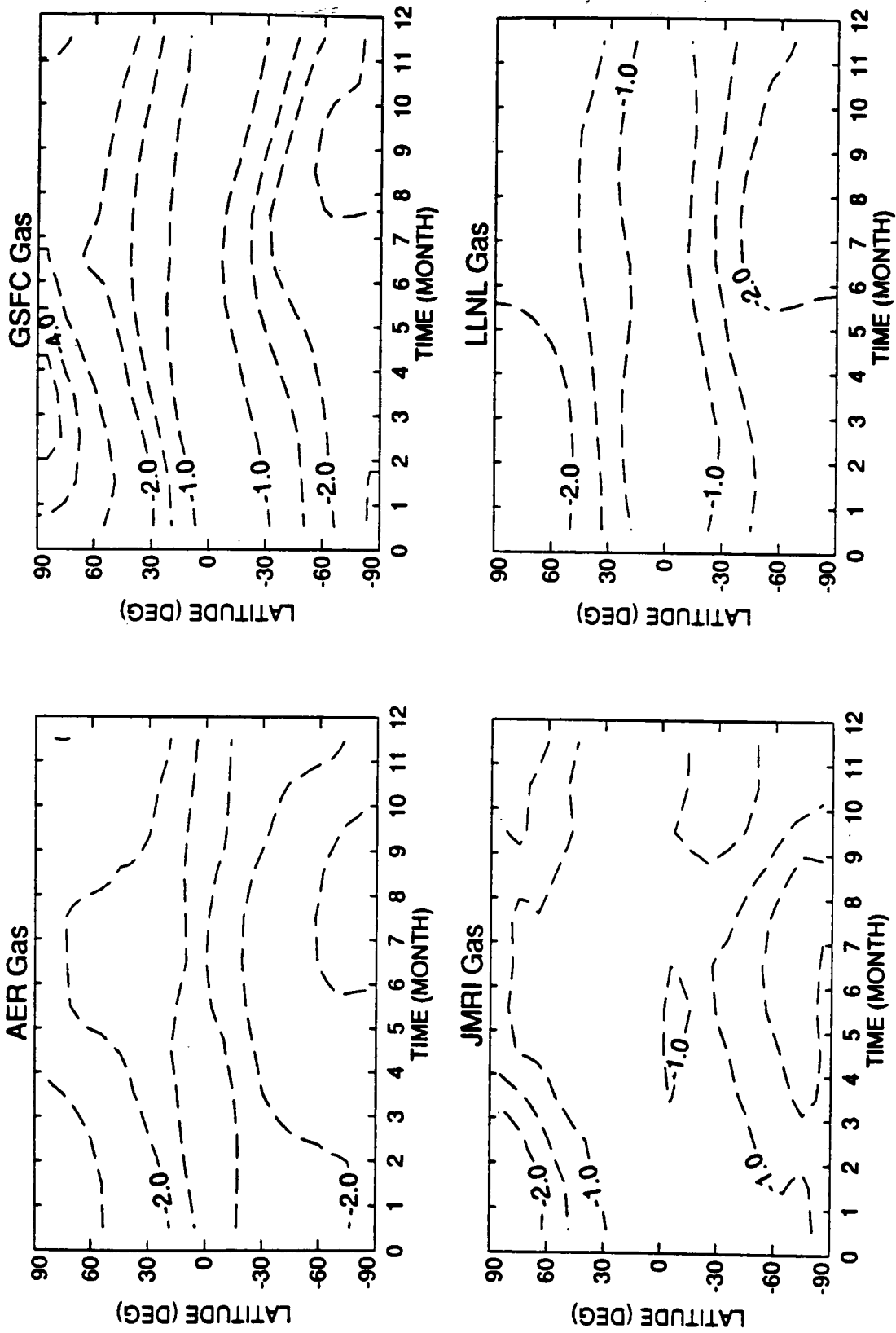


Figure 8-9a Change in column ozone abundances (percent) from 1980 to 2000 based on modeled Scenario A.

FUTURE CI-Br Loading AND OZONE DEPLETION

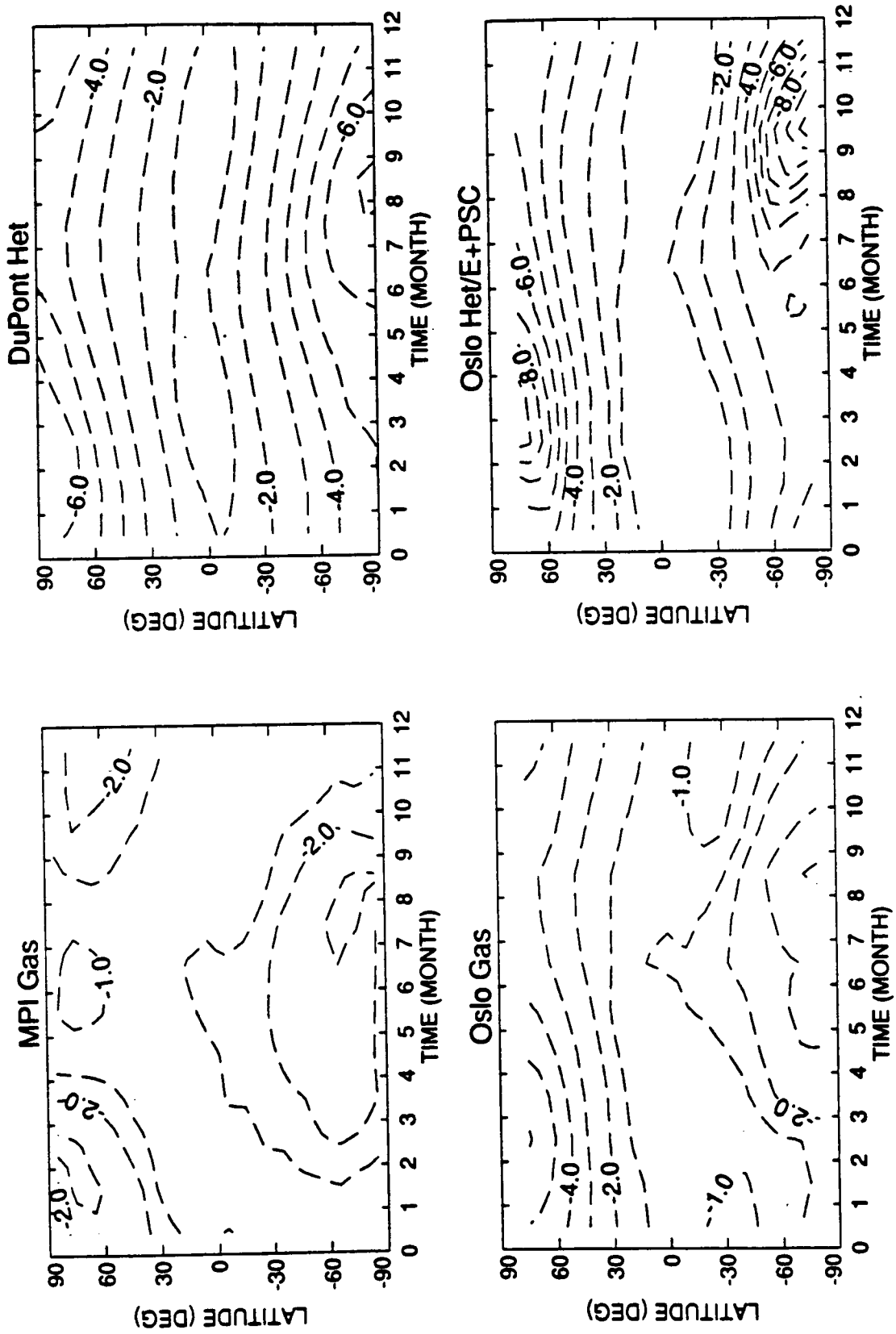


Figure 8-9b Change in column ozone abundances (percent) from 1980 to 2000 based on modeled Scenario A.

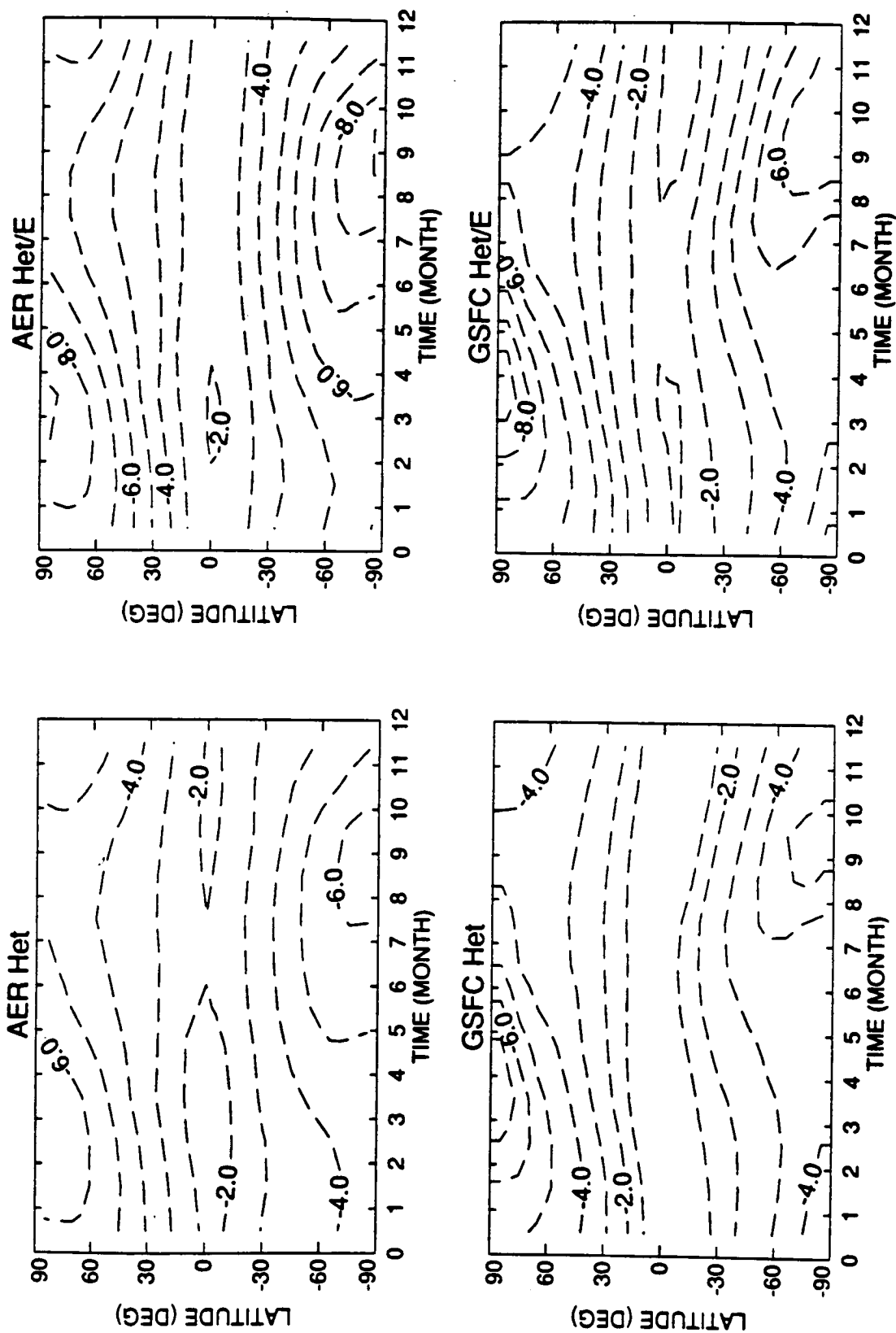


Figure 8-9c Change in column ozone abundances (percent) from 1980 to 2000 based on modeled Scenario A.

FUTURE Cl-Br LOADING AND OZONE DEPLETION

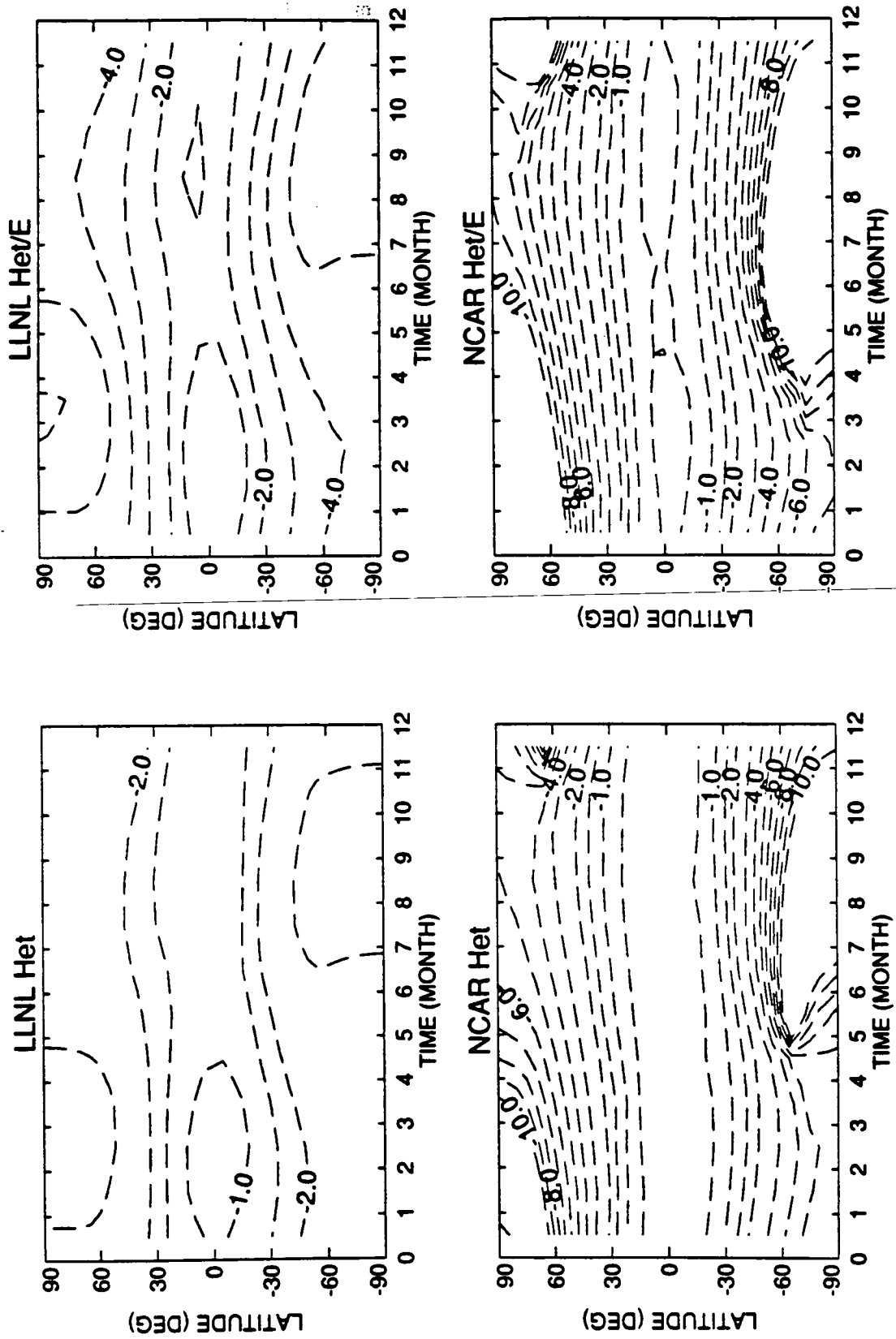


Figure 8-9d Change in column ozone abundances (percent) from 1980 to 2000 based on modeled Scenario A.

The largest differences among the model predictions occurs for the longest time interval, year 1980 to year 2050, where the changes in trace gases are largest. Under these circumstances, the predictions for 2050 depend on competing changes in Cl_y , Br_y , NO_y (through N_2O), CH_4 , and stratospheric temperatures (through CO_2 and O_3 changes). Model predictions for the full range of chemical formulations are shown in Figure 8-11. The GAS models agree that perturbations in the tropics should be small, usually less than 1 percent; however, at mid-latitudes and the poles the predictions range from -3 to +4 percent. The HET models all show increases in column ozone of about 2 to 4 percent. This increase is due in part to the choice of 1980 as the reference year, as noted above. Several PSC models included the effects of chemical processing by PSCs (independently, since no method was agreed upon for these scenarios). They also predict a general increase in ozone column everywhere except in the Antarctic spring where the ozone hole still exists, but additional losses relative to the year 1980 are limited.

8.4.3 Peak Chlorine Loading and Integrated Halocarbon Effects

Both predictions and observations indicate that rising chlorine levels in the stratosphere are likely to lead to more extensive and deeper ozone loss. The apparently nonlinear response of ozone to chlorine makes us focus on the maximum levels of stratospheric chlorine. In this section we examine the atmospheric chlorine loading of halocarbons (CL) as a surrogate for chlorine-catalyzed ozone loss in the stratosphere (Prather and Watson, 1990). We recognize that tropospheric chlorine loading from halocarbons will be realized as stratospheric Cl_y with a time delay of 2-4 years and with some systematic reductions in absolute amount due to incomplete oxidation of the halocarbon source gases (*i.e.*, Cl_y is always less than CL). Thus CL is a conservative measure (*i.e.*, upper limit) of the amount of chlorine available to participate in ozone destruction.

Recent work on modeling and data analysis (see Chapter 6) has led to a better determination of the chemically active chlorine (Cl_y) in the lower, middle latitude stratosphere, where the bulk of the ozone loss is now observed. A specific fraction of each halocarbon source molecule is assumed to have been

photochemically destroyed and thus contribute to the total Cl_y in the lower stratosphere. Some halocarbons, particularly those with a $-\text{CCl}_3$ segment, are readily photolyzed in the lower stratosphere and thus release almost all of their Cl atoms to Cl_y , (see notes to Table 8-B). Others, such as CHF_2Cl , are estimated to have remained mostly intact and release only about a third of their chlorine loading as Cl_y . We define free chlorine (FC), an estimate of Cl_y in the lower stratosphere, as the weighted sum of the chlorine loadings of the source gases.

Bromine-containing halocarbons release active bromine (Br_y) in the stratosphere, which has been measured as BrO and is calculated to contribute significantly to ozone loss over the past decade (see also Chapters 4 and 6). The relative importance, in terms of ozone destruction, of one molecule of Br_y to that of one molecule of Cl_y (defined as α in Chapter 6) varies by more than a factor of 10, depending on the altitude and the absolute amounts of Cl_y present. (When ClO concentrations are high, the ClO -dimer rapidly catalyzes ozone loss and the BrO - ClO cycle is less important; similarly at higher altitudes, the ClO - O reaction dominates. Bromine is relatively most important in the lower stratosphere when ClO levels are less than about 1 ppbv.) Averaging over the lower stratosphere, model results give α ranging from 30 to 120, and we select a value of 40 here to define the free halogen (FH) content of the lower stratosphere (see Table 8-B). Based on observations (see Chapter 6), bromine atoms in the halons and methyl bromide are assumed to be available as stratosphere Br_y , and thus a large part of the halogen-driven destruction of ozone in the lower stratosphere (about 1 ppbv of FH) is due to bromine, predominantly methyl bromide.

The peak chlorine loading is expected to occur between 1995 and 2000 depending on the details of the phaseout of industrial halocarbons. The analysis here pushes the simple model for halogen loading to its limit of credibility, *i.e.*, the model does not include banking of production for later emission and uses a one-year time step. Therefore, we must use these results as a guide to the relative changes in chlorine loading in response to different policy options rather than as a prediction of absolute year-by-year chlorine loading. All of the basic halocarbon scenarios (A, B, and C) show the same peak CL of about 4.13 ppbv, which is 0.05 ppbv greater than Scenario M (absolute global compliance with the protocol, no delays or

FUTURE CI-Br LOADING AND OZONE DEPLETION

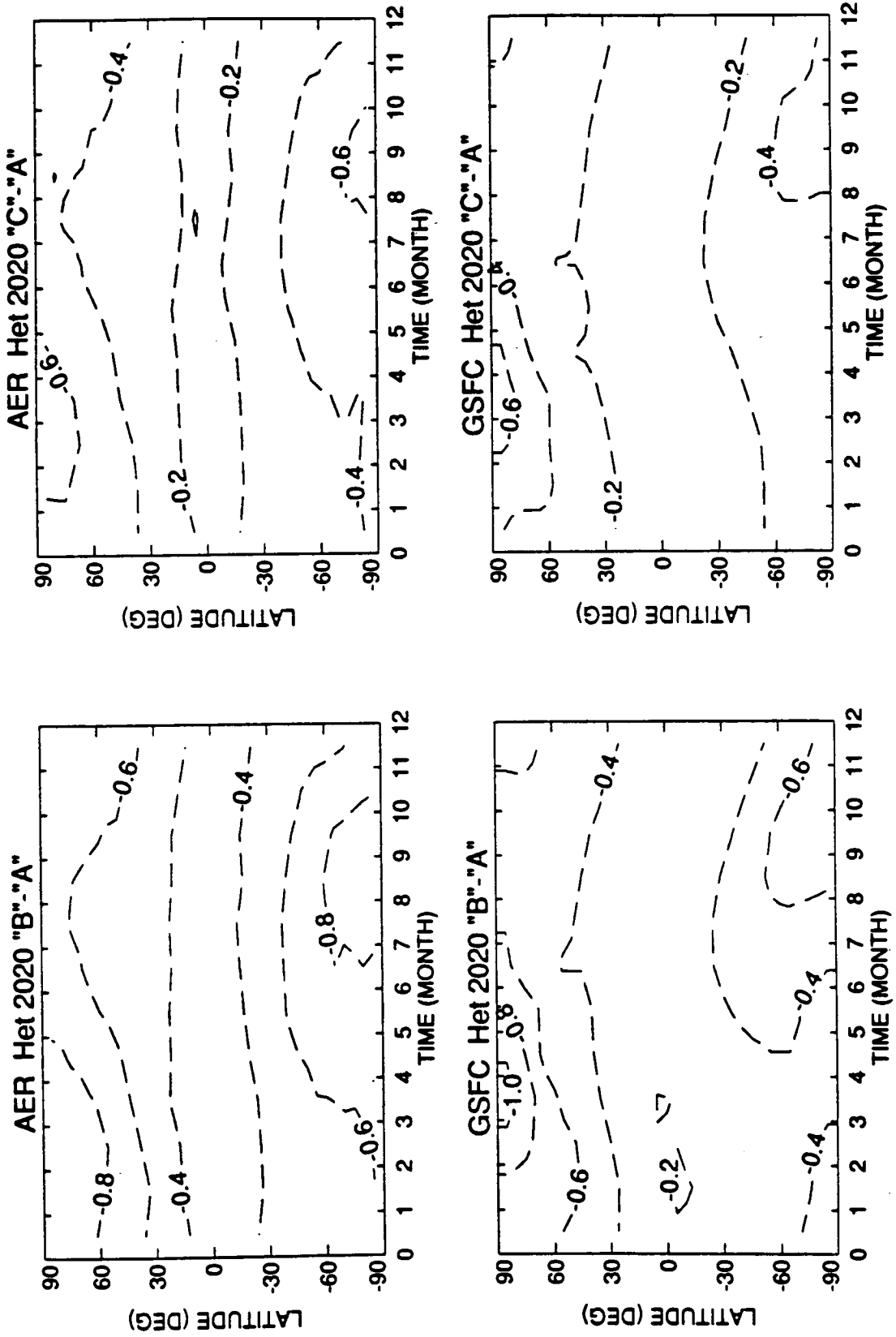


Figure 8-10 Difference in column ozone (percent) between Scenario A, B, & C at 2020 from the AER and GSFC models.

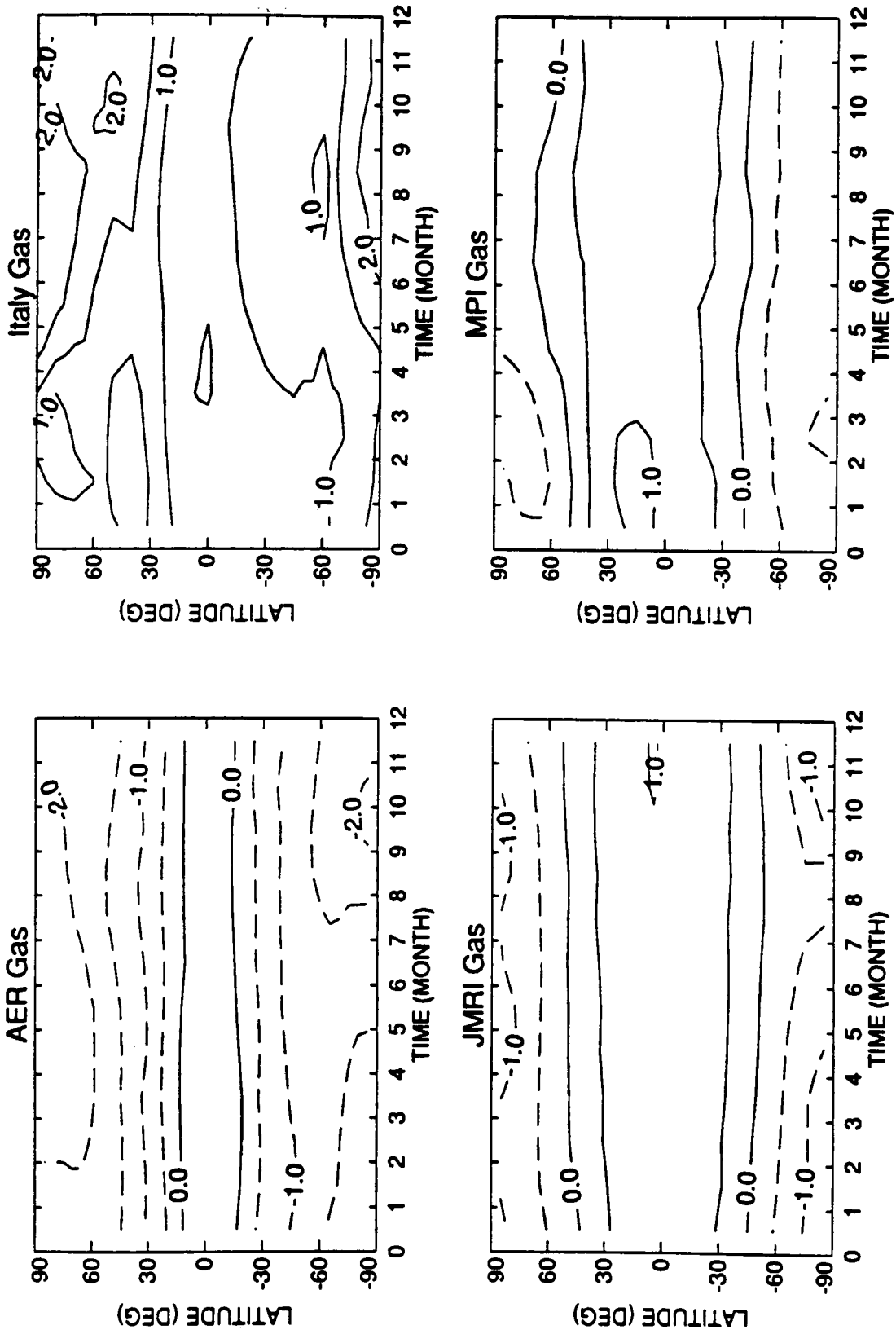


Figure 8-11a Change in column ozone abundances (percent) from 1980 to 2050 based on modeled Scenario A.

FUTURE Cl-Br LOADING AND OZONE DEPLETION

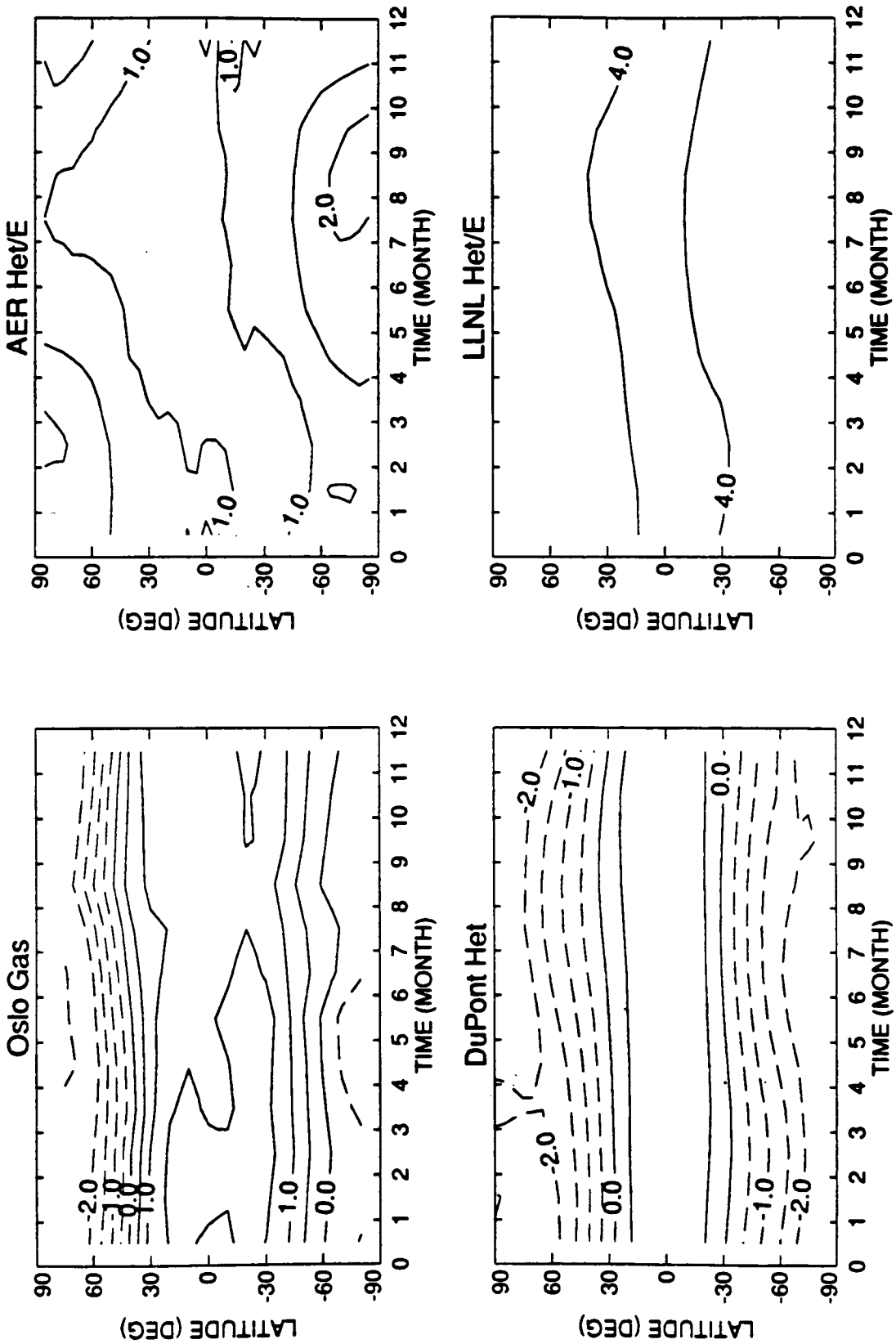


Figure 8-11b Change in column ozone abundances (percent) from 1980 to 2050 based on modeled Scenario A.

FUTURE CI-Br LOADING AND OZONE DEPLETION

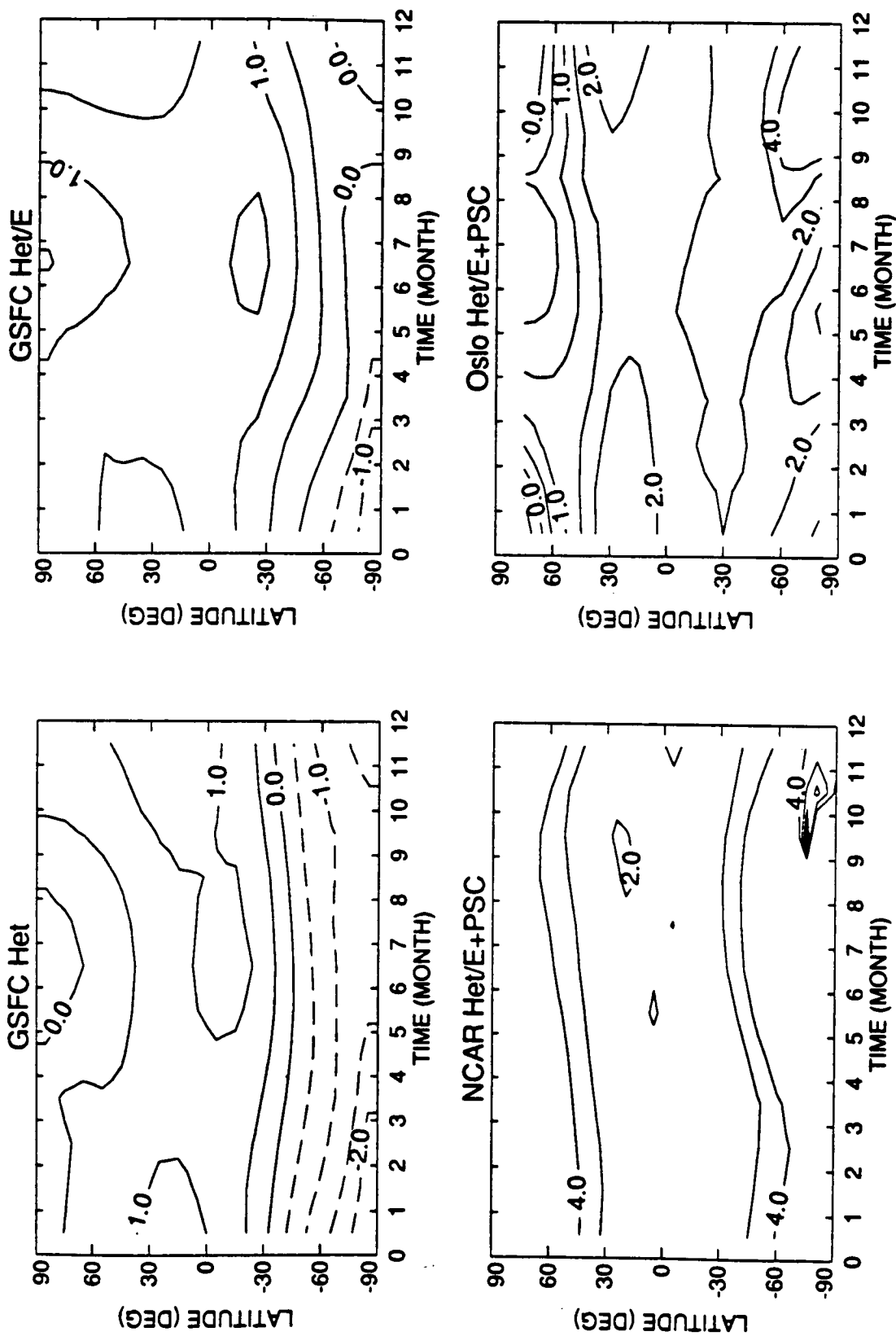


Figure 8-11c Change in column ozone abundances (percent) from 1980 to 2050 based on modeled Scenario A.

FUTURE Cl-Br LOADING AND OZONE DEPLETION

substitutions, and eventual phaseout of all chlorinated halocarbons not specifically in the current protocol). A wider variety of options, defined in Table 8-B, is considered here in order to focus on the details of the maximum CL, FC, and FH. The peak CL in the late 1990s may vary over a range of 0.2 ppbv in response to a wide variety of options for halocarbon phaseouts and HCFC substitution. A significant reduction in peak CL (FC and FH also) can be achieved with accelerated phase-out schedules of CFCs, carbon tetrachloride, and methyl chloroform. The times at which CL falls below 3 and 2 ppbv can be shifted by at most 10 years with such an acceleration of the phaseout.

It is important to recognize that the environmental impact of ozone loss, with corresponding enhancement of ultraviolet-B (UVB) exposure, may be cumulative over the years with high ozone depletion. Thus, we define an integral of the chlorine loading (units of ppbv-year) above some threshold as a surrogate for the chronic UVB exposure. The choice of threshold is arbitrary, and a low value such as 1 ppbv would require integration out beyond the 21st century. We focus on the apparently rapid loss of ozone during the 1980s (see Chapter 2), and select 1985 as the threshold year, integrating from 1985 until the values of CL, FC, and FH fall below 3.00, 2.45, and 3.18 ppbv, respectively. The integral CL is more sensitive to the differences between certain policy options: heavy substitution with HCFCs can increase this number by at most 20 percent, whereas accelerated phaseouts can reduce it by as much as 50 percent. Acceleration of the halon phaseout by 3 years would reduce peak bromine loading by 1 pptv (about 4 percent), and thus FH by 0.04 ppbv. Stringent controls on current use of HCFC-22, or on substitution with alternative HCFCs, would not significantly reduce peak chlorine, but would accelerate the decay in chlorine loading in the decades following the peak. Following phaseout of halocarbons, the free chlorine levels drop more rapidly than the chlorine loading because species that contribute most to FC have shorter stratospheric lifetimes (*e.g.*, CFCl_3 , CCl_4), whereas the longer-lived CFCs have FC/CL ratios much less than 1. Scenarios in Table 8-B show the extreme sensitivity of integral quantities to a range of halocarbon phaseout schedules.

8.5 OPTIONS AND ISSUES TO 2100

These calculations were performed using both the traditional gas phase chemical models and a new heterogeneous formulation that includes the reactions of N_2O_5 and ClONO_2 on the background sulfate aerosols. A few models included a parameterization of PSC chemistry, but no agreed-upon approach was taken. Although the new HET models were better able to simulate the recent trends in column ozone over the mid-latitudes, they still do not predict *ab initio* the Antarctic ozone hole. (Furthermore, the current trends might also be explained by an extension of the PSC chemistry mixing to mid-latitudes.) Nevertheless, it is clear from laboratory studies that some form of heterogeneous chemistry on sulfate aerosols should be part of stratospheric models. Based on three-dimensional analysis and model studies (*e.g.*, Lefèvre *et al.*, 1991; Cariolle *et al.*, 1990) it is unlikely that a strictly two-dimensional formalism is adequate to reproduce the chemical processes occurring on PSCs. Zonal asymmetries in PSCs as well as dilution and chemical propagation of O_3 loss from polar regions to mid-latitudes occurs in dimensions and spatial scale not resolved by the current assessment models (*e.g.*, Juckes and McIntyre, 1987; Atkinson *et al.*, 1989; Tuck, 1989; Prather and Jaffe, 1990).

We chose not to examine scenarios for chlorine and bromine loading that continued to increase beyond 4.1 ppbv in 1995. Had we done so, the implications for ozone loss would be severe: the predictions for the year 2000 show that ozone losses may be more than linearly proportional to Cl_y increases, and depletions that were initially limited to the winter pole now extend towards the equator. If halocarbon regulations admit a scenario whereby chlorine increases beyond 5 ppbv, then this assessment must be revisited. It is important to develop a scientifically based measure of cumulative ozone depletion and to relate this to halocarbon loading. In the models and scenarios used here, the impact of bromine increases was not singled out. It appears small, but this may be a major oversight since the greatest effect of Br_y -catalyzed ozone loss would be in PSC chemistry, which we have more difficulty simulating in two-dimensional models.

By the year 2050, we may expect that some residual ozone depletion remains (*e.g.*, the Antarctic

ozone hole, plus some mid-latitude losses), due to chlorine since the tropospheric loading is still expected to exceed 2 ppbv. The model predictions shown here paint a rosier picture by virtue of the choice in trends for N_2O and CH_4 giving predominantly ozone increases relative to the year 1980. One key uncertainty is the importance of N_2O increases: in the AER GAS model, the resulting NO_y increases lead to a 1 to 4 percent additional decrease in column ozone by the year 2050, but in the HET model the impact of N_2O is at most 1 percent. These results point out the importance of the many influences on stratospheric ozone. The greatest uncertainty in predicting ozone in the years 2050 to 2100, providing something like the current Montreal Protocol is in place, will be in predicting the changes in other trace gases (N_2O , CH_4) and climate (CO_2).

REFERENCES

- AFEAS, Alternative Fluorocarbon Environmental Acceptability Study, *Scientific Assessment of Stratospheric Ozone: 1989, Vol. II Appendix: AFEAS Report*, Global Ozone Research and Monitoring Project, Report No. 20, World Meteorological Organization, Geneva, 1990.
- Atkinson, R.J., W.A. Matthews, P.A. Newman, and R.A. Plumb, Evidence of the middle latitude impact of the Antarctic ozone depletion, *Nature*, **340**, 290–293, 1989.
- Bruehl, C.P., and P.J. Crutzen, Scenarios of possible changes in atmospheric temperatures and ozone concentrations due to man's activities, estimated with a one-dimensional coupled photochemical climate model, *Climate Dynamics*, **2**, 173–203, 1988.
- Cariolle, D., A. Lasserre-Bigorry, J.F. Royer, and J.F. Geleyn, A general circulation model simulation of the springtime Antarctic ozone decrease and its impact on mid-latitudes, *J. Geophys. Res.*, **95**, 1883–1898, 1990.
- Cunnold, D.M., R.G. Prinn, R.A. Rasmussen, P.G. Simmonds, F.N. Alyea, C.A. Cardelino, A.J. Crawford, P.J. Fraser, and R.D. Rosen, Atmospheric lifetime and annual release estimates for $CFCl_3$ and CF_2Cl_2 from 5 years of data, *J. Geophys. Res.*, **91**, 10797–10817, 1986.
- DeMore, W.B., S.P. Sander, R.F. Hampson, M.J. Kurylo, D.M. Golden, C.J. Howard, A.R. Ravishankara, and M.J. Molina, Chemical kinetics and photochemical data for use in stratospheric models, *JPL Publ.* 90–1, 1990.
- Derwent, R.G., and A. Volz-Thomas, The tropospheric lifetimes of halocarbons and their reactions with OH radicals: an assessment based on the concentration of ^{14}CO , in *Alternative Fluorocarbon Environmental Acceptability Study, Scientific Assessment of Stratospheric Ozone: 1989, vol. II, Appendix*, Global Ozone Research and Monitoring Project, Rep. 20, 125–146, World Meteorological Organization, 1990.
- Douglass, A.R., C.H. Jackman, and R.S. Stolarski, Comparison of model results transporting the odd nitrogen family with results transporting separate odd nitrogen species, *J. Geophys. Res.*, **94**, 9862–9872, 1989.
- Hofmann, D.J., and S. Solomon, Ozone destruction through heterogeneous chemistry following the eruption of El Chichón, *J. Geophys. Res.*, **94**, 5029–5041, 1989.
- Holton, J.R., On the global exchange of mass between the stratosphere and troposphere, *J. Atmos. Sci.*, **47**, 392–395, 1990.
- IPCC, Intergovernmental Panel on Climate Change, J.T. Houghton, G.J. Jenkins and J.J. Ephraums, eds., *Climate Change: The IPCC Scientific Assessment*, 365 pp., U. Cambridge Press, 1990.
- Isaksen, I.S.A., B. Rognerud, F. Stordal, F. Coffey, and W.G. Mankin, Studies of arctic stratospheric ozone in a 2D model including some effects of zonal asymmetries, *Geophys. Res. Lett.*, **17**, 557–560, 1990.
- Jackman, C.H., R.K. Seals Jr., and M.J. Prather, eds., 2D Intercomparison of stratospheric models, *NASA Conference Publication*, CP–3042, 608 pp, 1989a.
- Jackman, C.H., A.R. Douglass, P.D. Guthrie, and R.S. Stolarski, The sensitivity of total ozone and ozone perturbation scenarios in a 2D model due to dynamical inputs, *J. Geophys. Res.*, **94**, 9873–9887, 1989b.
- Jackman, C.H., A.R. Douglass, R.B. Rood, R.D. McPeters, and P.E. Meade, Effect of solar proton events on the middle atmosphere during the past two solar cycles as computed using a 2D model, *J. Geophys. Res.*, **95**, 7417–7428, 1990.
- Jukes, M.N., and M.E. McIntyre, A high-resolution one-layer model of breaking planetary waves in the stratosphere, *Nature*, **328**, 590–596, 1987.
- Ko, M.K.W., N.D. Sze, M. Livshits, M.B. McElroy, and J.A. Pyle, The seasonal and latitudinal behaviour of trace gases and O_3 as simulated by a 2D model of the atmosphere, *J. Atmos. Sci.*, **41**, 2381–2408, 1984.

FUTURE Cl-Br LOADING AND OZONE DEPLETION

- Ko, M.K.W., K.K. Tung, D.K. Weisenstein, and N.D. Sze, A zonal mean model of stratospheric tracer transport in isentropic coordinates: numerical simulations for nitrous oxide and nitric acid, *J. Geophys. Res.*, *90*, 2313–2329, 1985.
- Ko, M.K.W., N.D. Sze, and D.K. Weisenstein, The roles of dynamical and chemical processes in determining the stratospheric concentration of ozone in 1D and 2D models, *J. Geophys. Res.*, *94*, 9889–9896, 1989.
- Krecov, G., and S. Zvenigorodsky, Optical models of the Middle Atmosphere, Ac.Sci.Publ. Nauka, 345 pp., 1990.
- Lefèvre, F., D. Cariolle, S. Muller, and F. Karcher, Total ozone from the TIROS operational vertical sounder during the formation of the 1987 "ozone hole," *J. Geophys. Res.*, *96*, 12893–12911, 1991.
- Mahlman, J.D., H. Levy II, and W.J. Moxim, Three-dimensional tracer structure and behavior as simulated in two ozone precursor experiments, *J. Atmos. Sci.*, *37*, 655–685, 1980.
- Montreal Protocol on Substances that Deplete the Ozone Layer, Final Act, UNEP, 1987, revised 1990, London.
- Penkett, S.A., B.M.R. Jones, M.J. Rycroft, and D.A. Simmons, An interhemispheric comparison of the concentration of bromine compounds in the atmosphere, *Nature*, *318*, 550–553, 1985.
- Pitari, G., and G. Visconti, Two-dimensional tracer transport: derivation of residual mean circulation and eddy transport tensor from a three-dimensional model data set, *J. Geophys. Res.*, *90*, 8019, 1985.
- Pitari, G., and G. Visconti, Ozone trend in the Northern Hemisphere: a numerical study, *J. Geophys. Res.*, *96*, 10931–10940, 1991.
- Pitari, G., G. Visconti, and V. Rizi, Sensitivity of stratospheric ozone to heterogeneous chemistry on sulfate aerosols, *Geophys. Res. Lett.*, *18*, 833–836, 1991.
- Prather, M.J., M.B. McElroy, and S.C. Wofsy, Reductions in ozone at high concentrations of stratospheric halogens, *Nature*, *312*, 227–231, 1984.
- Prather, M.J., and C. M. Spivakovsky, Tropospheric OH and the lifetimes of hydrochlorofluorocarbons (HCFCs), *J. Geophys. Res.*, *95*, 18723–18729, 1990.
- Prather, M., and A. Jaffe, Global impact of the Antarctic ozone hole: chemical propagation, *J. Geophys. Res.*, *95*, 3473–3492, 1990.
- Prather, M.J., and R. T. Watson, Stratospheric ozone depletion and future levels of atmospheric chlorine and bromine, *Nature*, *334*, 729–734, 1990.
- Prinn, R., D. Cunnold, R. Rasmussen, P. Simmonds, F. Alyea, A. Crawford, P. Fraser, and R. Rosen, Atmospheric trends in methyl chloroform and the global average for the hydroxyl radical, *Science*, *238*, 946–950, 1987.
- Prinn, R., D. Cunnold, P. Simmonds, F. Alyea, R. Boldi, A. Crawford, P. Fraser, D. Gutzler, D. Hartley, R. Rosen, and R. Rasmussen, Global average concentration and trend for hydroxyl radicals deduced from ALE/GAGE trichloroethane (methyl chloroform) data for 1978–1990, *J. Geophys. Res.*, *97*, 2445–2461, 1992.
- Rodriguez, J.M., K. W. Ko, and N. D. Sze, Role of heterogeneous conversion of N_2O_5 on sulphate aerosols in global ozone losses, *Nature*, *352*, 134–137, 1991.
- Schmidt, U., and A. Khedim, *In situ* measurements of CO_2 in the winter Arctic vortex and at the middle latitude s: an indicator of the 'age' of stratospheric air, *Geophys. Res. Lett.*, *18*, 763–766, 1991.
- Schmidt, U., R. Bauer, A. Khedim, E. Klein, G. Kullessa, and C. Schiller, Profile observations of long-lived trace gases in the Arctic Vortex, *Geophys. Res. Lett.*, *18*, 767–770, 1991.
- Spivakovsky, C.M., S.C. Wofsy and M.J. Prather, A numerical method for parameterization of atmospheric photochemistry: computation of tropospheric OH, *J. Geophys. Res.*, *95*, 18433–18439, 1990.
- Stordal, F., I.S.A. Isaksen, and K. Horntveth, A diabasic circulation 2D model with photochemistry: simulations of ozone and long-lived tracers with surface sources, *J. Geophys. Res.*, *90*, 5757–5776, 1985.
- Tolbert, M.A., M.J. Rossi, and D.M. Golden, Heterogeneous interactions of $ClONO_2$, HCl and HNO_3 with sulfuric acid surfaces at stratospheric temperatures, *Geophys. Res. Lett.*, *15*, 847–850, 1988.
- Tuck, A.F., Synoptic and chemical evolution of the Antarctic vortex in late winter and early spring, 1987, *J. Geophys. Res.*, *94*, 11687–11737, 1989.
- WMO, *Report of the International Ozone Trends Panel: 1988*, Global Ozone Research and Monitoring Project, Report No. 18, World Meteorological Organization, 1990b.
- WMO, *Scientific Assessment of Stratospheric Ozone: 1989, Vol. I*, Global Ozone Research and Monitoring Project, Report No. 20, World Meteorological Organization, 1990b.